

Shear Force Production in Dogs: Differential Force Production in the Forelimbs and Hindlimbs During Pulling

A Thesis

Presented in Partial Fulfillment of the Requirements for the

Degree of Master of Science

with a

Major in Biology

in the

College of Graduate Studies

University of Idaho

by

Ike Brown

Major Professor: Craig P. McGowan, Ph.D.

Committee Members: Joshua Bailey, Ph.D.; Jack Sullivan, Ph.D.

Department Chair: James J. Nagler, Ph.D.

December 2019

Authorization to Submit Thesis

This thesis of Ike E. Brown, submitted for the degree of Master of Science with a Major in Biology and titled "Shear Force Production in Dogs: Differential Force Production in the Forelimbs and Hindlimbs During Pulling," has been reviewed in final form. Permission, as indicated by the signatures and dates below, is now granted to submit final copies to the College of Graduate Studies for approval.

Major Professor: _____ Date: _____
Craig P. McGowan, Ph.D.

Committee Members: _____ Date: _____
John "Jack" M. Sullivan, Ph.D.

_____ Date: _____
Joshua P. Bailey, Ph.D.

Department Administrator: _____ Date: _____
James J. Nagler, Ph.D.

Abstract

Dogs are widely recognized as some of the best endurance athletes in the world. Much is known about their physiological specializations for endurance. However, we know much less about their mechanical specializations. One hypothesis is that the forward weight distribution found in dogs and in many other quadrupeds results in the decoupling of vertical and shear force production. In this study, I examine the differential distribution of shear forces between the forelimbs and the hindlimbs of dogs during active shear force production. I use pulling as a loading perturbation in order to achieve variable shear loading without the confounding variables of increasing velocity and altered limb angles that are associated with acceleration and incline studies. The results of this study showed that complete vertical and shear force decoupling between the forelimbs and the hindlimbs does not exist during submaximal shear force production. However, the distribution of propulsive shear force production is heavily biased towards the hindlimbs and remains so throughout active shear force production despite shifts in net shear force production. In addition, the results of this study indicate that the basic mechanics of shear force production are conserved in acceleration, incline locomotion, and pulling.

Acknowledgements

I would like to thank my major professor, Dr. Craig McGowan, for his instruction and guidance throughout this process. Also, I would like to thank Dr. McGowan for seeing the good in things when they didn't go quite as planned. I would also like to thank my advising committee members, Dr. Jack Sullivan and Dr. Josh Bailey. Their advice and their willingness to help was a great benefit to this study, and I only wish I had taken fuller advantage of it. I would like to thank all of the members of the McGowan Lab for helping throughout this study, especially for the many times they came out to encourage somewhat skeptical dogs about the merits of pulling a sled across a couple of force plates. I would like to thank Dr. James Nagler, the department chair, for his support, as well as that of the staff and faculty of the University of Idaho Biology Department. Lastly, I would like to thank all of the dog owners, dogs, and mushers who willingly gave their time and advice without any incentive other than a sincere interest in science and some dog treats on the part of the dogs.

Table of Contents

Authorization to Submit Thesis	ii
Abstract	iii
Acknowledgements	iv
Table of Contents	v
List of Tables	vii
List of Figures	viii
List of Equations	x
Chapter 1: Shear Force Production in Dogs	1
Introduction.....	1
Canine Efficiency and Vertical and Shear Force Decoupling.....	1
The Strut and Lever Models of Locomotion.....	1
Vertical and Shear Force Decoupling During Active Shear Force Production.....	2
Objectives and Hypotheses	4
Materials and Methods	5
Experimental Animals	5
Experimental Setup	5
Experimental Protocol	6
Force Data.....	7
Force Plates	8
In-line Force Transducer.....	11
Video Data	12
Statistics	13
Results	14
Morphometrics and Kinematics	14
Ground Reaction Forces	17
Shear GRFs	18
Vertical GRFs.....	27
Resultant GRFs.....	33
Discussion.....	36
Objective 1	36
Shear Force Production.....	36
Vertical Force Production	37
Objective 2.....	38

Resultant GRF Angle.....	39
Resultant GRF Magnitude	39
Relation to Other Studies	39
Conclusions.....	40
Limitations	41
Subject Limitations.....	41
Equipment Limitations	42
Methodological Limitations	42
Literature Cited	44

List of Tables

Table 1.1. Subject descriptions	5
Table 1.2. Morphometrics.. ..	14

List of Figures

Figure 1.1. Outdoor runway and camera setup.	6
Figure 1.2. Binocular double beam spring element design.....	9
Figure 1.3. Stride frequency vs whole animal net shear over the course of the stride.	14
Figure 1.4. Stride length vs whole animal net shear over the course of the stride.	15
Figure 1.5. Fore and hind contact time vs whole animal net shear over the course of the stride.....	15
Figure 1.6. Fore and hind swing time vs whole animal net shear over the course of the stride.....	16
Figure 1.7. Mean x-velocity vs whole animal net shear over the course of the stride.	16
Figure 1.8. Whole animal net shear and vertical GRFs vs mean pulling load over the course of the stride.....	17
Figure 1.9. Whole animal net shear and vertical GRFs vs. mean pulling load over the course of the stride. Shear and vertical forces are given as % of their unloaded mean.	18
Figure 1.10. Mean forelimb, hindlimb, and whole animal net shear (Sum) GRFs vs. mean pulling load over the course of the stride. All conditions.	19
Figure 1.11. Mean forelimb, hindlimb, and whole animal net shear (Sum) GRFs vs. mean pulling load over the course of the stride. Loaded conditions.....	19
Figure 1.12. Mean forelimb and hindlimb net shear GRFs vs mean whole animal net shear GRF over the course of the stride	20
Figure 1.13. Mean forelimb and hindlimb braking GRFs vs mean pulling load over the course of the stride.....	21
Figure 1.14. Mean forelimb and hindlimb braking GRFs vs mean whole animal net shear GRF over the course of the stride	22
Figure 1.15. Mean forelimb and hindlimb propulsive GRFs vs mean pulling load over the course of the stride	23
Figure 1.16. Mean forelimb and hindlimb propulsive GRFs vs mean whole animal net shear GRFs over the course of the stride.....	24
Figure 1.17. Braking-propulsion bias vs mean pulling load over the course of the stride	25
Figure 1.18. Braking-propulsion bias vs whole animal net shear over the course of the stride.....	25
Figure 1.19. Percent of propulsive and braking forces provided by the forelimbs vs pulling load over the course of the stride	26
Figure 1.20. Percent of propulsive and braking forces provided by the forelimbs vs whole animal net shear over the course of the stride.....	26
Figure 1.21. Mean fore, hind, and summed fore and hind vertical GRFs vs. mean pulling load over the stride.	28
Figure 1.22. Mean fore, hind, and summed fore and hind vertical GRFs vs. mean whole animal net shear GRF over the stride.	28
Figure 1.23. % vertical GRF provided by the fore and hindlimbs vs mean pulling load over the stride.	29

Figure 1.24. % vertical GRF provided by the fore and hindlimbs vs mean whole animal net shear GRF over the stride.	30
Figure 1.25. Duty factor at the forelimb and hindlimb vs mean pulling load over the stride.	30
Figure 1.26. Duty factor at the forelimb and hindlimb vs mean whole animal net shear GRF over the stride.	31
Figure 1.27. Peak vertical GRFs at the forelimb and hindlimb vs mean pulling load over the stride.	32
Figure 1.28. Peak vertical GRFs at the forelimb and hindlimb vs mean whole animal net shear GRF over the stride.	32
Figure 1.29. Fore, hind, and whole animal resultant GRF angle vs mean pulling load over the stride.	33
Figure 1.30. Fore, hind, and whole animal resultant GRF angle vs mean whole animal net shear GRF over the stride.	34
Figure 1.31. Fore, hind, and summed fore and hind resultant GRF magnitude vs mean pulling load over the stride.	35
Figure 1.32. Fore, hind, and summed fore and hind resultant GRF magnitude vs mean whole animal net shear GRF over the stride.	35

List of Equations

Equation 1.1. Maximum strain in a connected cantilever beam	10
Equation 1.2. Maximum strain in a connected double cantilever beam	10
Equation 1.3. Maximum strain in a ring in tension	11

Chapter 1: Shear Force Production in Dogs

Introduction

Canine Efficiency and Vertical and Shear Force Decoupling

Dogs are capable of incredible endurance¹⁻¹³. Wolves have been recorded traveling almost 100 km in a single day⁴. Similarly, arctic foxes can travel 90 km/day in sustained travel⁵. Although domestic dogs are separated from their wild relatives by thousands of years of domestication, many breeds maintain the athletic abilities of their wild counterparts. Sled dogs are arguably the best endurance athletes in the world^{7, 13}, and are capable of traveling over 150 km/day even while pulling a loaded sled⁶. Many studies have demonstrated that dogs are physiologically specialized for endurance^{3,8-10,12-13}. However, our knowledge of their mechanical specializations is much less complete.

It is known that the trot is the most energetically efficient gait for dogs¹⁴⁻¹⁶. This is in part due to the transfer between kinetic energy and elastic energy¹⁷⁻²⁰. In addition, the forward weight distribution of dogs may also facilitate endurance. Usherwood and Wilson demonstrated that dogs are able to maintain top speeds while turning despite the increased limb forces that are incurred due to centripetal acceleration²¹. They hypothesized that the forward weight distribution found in dogs enables the decoupling of vertical and shear force production. This same effect may be important for submaximal locomotion. If vertical force production is divorced from shear force production to some extent, then this could facilitate increased endurance because the musculature which is providing the forward propulsion is not being taxed by the need to support body weight. However, the degree to which this decoupling persists during submaximal locomotion is contested²²⁻²⁶. In this study, I use pulling as a loading regime in order to determine how the distribution of vertical and shear forces responds in order to produce an active shear force.

The Strut and Lever Models of Locomotion

Central to the idea of vertical and shear force decoupling are the strut and lever models of locomotion. Gray 1944 presents a model of tetrapod locomotion as a fully integrated system in which the functions of individual muscles and bones are coordinated with the function of the musculoskeletal system as a whole²⁷. Among Gray's primary contributions to our understanding of biomechanics are the strut and lever models of legged locomotion. The strut model describes the limb as an extensible strut in which the resultant ground reaction force (GRF) is directed through the proximal limb joint²⁷⁻²⁹. Under these conditions, all GRFs go directly towards restoring the body's

position and any additional shear forces required are produced by the intrinsic limb muscles acting to extend the limb. Furthermore, under the strut model no moments are generated about the proximal limb joint. In contrast, the lever model describes the limb as a lever in which force is produced via active contraction about the proximal limb joint. Under these conditions, the resultant GRF passes in front of the proximal limb joint. Although this prevents some GRFs from acting to restore the body's position, it allows for greater shear force production than is possible through limb extension alone²¹⁻²⁹.

In dogs, as well as in most other cursorial quadrupeds, the forelimbs appear to function as struts while the hindlimbs function as levers during steady state locomotion^{23,30}. This has been borne out by studies of both resultant GRFs and proximal retractor muscle activity^{23,30-31}. Results of these studies are consistent with vertical and shear force decoupling between the forelimbs and the hindlimbs because the strut model of locomotion redirects GRFs towards body support while the lever model of locomotion maximizes shear force production. By acting as a strut, the forelimbs are able to harness GRFs to restore vertical position while also avoiding generating moments about the shoulder. Meanwhile, the hindlimbs are able to utilize their extensive proximal retractor musculature in order to produce shear forces via lever type action.

Vertical and Shear Force Decoupling During Active Shear Force Production

While the idea of vertical and shear force decoupling appears to apply during steady state locomotion, the issue is complicated by studies which examine active shear force production. In an ideal system, no shear force production is required during steady state locomotion outside of that needed to redirect the limbs during swing phase. Considering this, there is little opportunity for dogs to benefit from vertical and shear force decoupling unless this decoupling also operates during active shear force production. To date, the majority of studies of active shear force production by quadrupeds have focused on either acceleration or inclines as loading perturbations^{24,25,32,33}. These studies contradict the vertical and shear force decoupling hypothesis by showing that the distribution of vertical and shear force production between the forelimbs and the hindlimbs shifts during acceleration and incline locomotion.

Lee 1999 explains this shift as a mechanism for balancing the tipping moment generated at the hip by shear force production²⁵. While this explanation is cogent, it is important to note that given the nature of levers, it is inevitable that some vertical force production accompanies any shear force produced by lever-like retraction at the hip. Furthermore, this explanation only accounts for the shift in vertical force production, not in shear force production. Complicating things further, neither acceleration nor inclines are pure shear force perturbations. Acceleration involves increasing speed which entails increasing either stride length or stride frequency. Inclines, on the other hand, alter the

position of the center of mass and involve changing limb angles. These confounding variables make it difficult to ascertain the root cause of shifts in vertical and shear force production.

An alternative to using acceleration or inclines to assess shear force production is to use pulling. Pulling allows the direct manipulation of external shear force demand while avoiding many of the confounding variables associated with acceleration and inclines. Furthermore, pulling allows one to easily set the shear load without significantly altering other factors. With acceleration and incline studies, increasing the shear load can only be accomplished by either increasing acceleration or increasing the grade, both of which magnify confounding variables. To my knowledge, only one series of studies has used pulling as a perturbation to investigate differential fore and hindlimb activity. Carrier et al. 2006 is the first in a series of 5 papers that investigate EMG activity of the extrinsic appendicular muscles under a variety of loading conditions^{22,23}. These studies found that during steady state locomotion, the proximal retractor muscles of the forelimbs were inactive throughout stance while the proximal retractor muscles of the hindlimbs were active during stance. This supports the decoupling of vertical and shear force production through the division of labor between the forelimbs and the hindlimbs. However, when an external shear load was applied through a rearward directed pull, the forelimb proximal retractor muscles became active during stance. This concurs with acceleration and incline studies in showing that the decoupling of vertical and shear force production appears to be reduced during active shear force production.

These results would appear to indicate that the redistribution of vertical and shear forces between the forelimbs and the hindlimbs may be a fundamental aspect of active shear force production. If this is the case, then it would indicate that any benefit derived from vertical and shear force decoupling is inversely related to the demand for shear force production. Although EMG studies are informative, there are several unknowns which must still be addressed before a verdict can be reached regarding the decoupling of vertical and shear force production during submaximal locomotion. Specifically, while EMG studies quantify when a muscle is active, they cannot predict the magnitude of forces being developed or the degree to which these forces translate to resultant GRFs. The relationship between muscle activation and force development varies with the force-length and force-velocity relationships of muscle and is therefore nonlinear. Furthermore, the effect of muscle activity on GRFs depends on multiple factors including the activity of other muscles, both extrinsic and intrinsic, and the relative position of the limb and center of mass at the time of muscle activation. Beyond this, it is likely that any shift in the distribution of vertical and shear force production occurs gradually. In order to address these issues, I combine direct shear force manipulation through pulling with direct GRF measurements. This will allow me to both isolate the

effects of active shear force production on the distribution of vertical and shear forces between the forelimbs and the hindlimbs and determine how this response scales with varying shear loads.

Objectives and Hypotheses

The goal of this study is to evaluate whether the decoupling of vertical and shear force production is maintained during active shear force production in submaximal locomotion and to determine whether this is accomplished through the action of the forelimbs as struts and the hindlimbs as levers.

Objective 1: Determine whether vertical and shear force decoupling between the forelimbs and the hindlimbs is maintained during active shear force production in submaximal locomotion. To achieve this, I will characterize shear force production during steady state trotting by dogs and determine how the distribution of vertical and shear forces respond in order to produce an active shear force across a range of pulling loads.

Hypothesis 1a: Vertical and shear force production by the forelimbs will not increase during pulling trials consistent with the division of labor between the fore and hind limbs with vertical force production at the forelimbs being decoupled from shear force production at the hindlimbs.

Hypothesis 1b: Shear force production by the hindlimbs will increase proportionally to the load in the pulling trials consistent with the division of labor between the fore and hind limbs with shear force production provided by the hindlimbs.

Objective 2: Determine whether the function of the forelimbs as struts and the hindlimbs as levers is maintained during active shear force production in submaximal locomotion. To achieve this, I will determine whether the resultant ground reaction force produced by the forelimbs and the hindlimbs is consistent with the strut or lever model of terrestrial locomotion and examine how the resultant ground reaction force shifts in response to a shear load.

Hypothesis 2a: The direction of the resultant ground reaction force at the forelimbs will be maintained during loaded trials consistent with continued strut type action at the forelimbs as opposed to lever type action in response to the shear load.

Hypothesis 2b: The direction of the resultant ground reaction force at the hind limbs will shift forward during loaded trials consistent with shear forces being produced at the hindlimbs via a lever type action.

The outcomes of this study will provide insight into a potential mechanical basis for canine endurance while also evaluating whether the model of the forelimbs as struts and the hindlimbs as levers can be maintained during active shear force production. Furthermore, the results of this study can be compared with previous studies on acceleration and inclines in order to determine which

findings are fundamental to shear force production and which are specific to a particular loading regime

Materials and Methods

Experimental Animals

Dogs were recruited from volunteer pet owners and collaboration agreements were obtained in accordance with IACUC protocol. Data were collected for 26 dogs; however, only data from 7 dogs was included in this study. Dogs ranged from 23 kg to 32 kg. Only mature dogs were used. Descriptive information for all subjects is listed in Table 1.

Table 1.1. Subject descriptions. The fraction of body weight supported by the forelimbs is denoted Fore/Aft.

Dog	Sex	Breed	Age (yrs)	BW (kg)	Fore/Aft
Lasso	Male	Border collie/Brittany mix	8.5	23.190	0.675
Trooper	Male	Border collie/Lab mix	3	31.727	0.675
Murphy	Male	Husky/Lab mix	1	31.226	0.577
Finnegan	Male	Husky/Lab mix	1	29.981	0.627
Hagrid	Male	Unknown	Unknown	28.272	0.517
Bear	Male	Weimaraner/Border collie/Pit bull mix	4	31.426	0.632
Kona	Female	Weimaraner/Border collie/Pit bull mix	4	23.899	0.615

Experimental Setup

The experimental setup consisted of two custom built force plates set in the ground in the middle of a 30m long outdoor runway (Figure 1.1). The surface of the runway varied over the course of data collection due to changing seasonal conditions. Initial data were collected with a runway surface of packed snow. Subsequent data were collected with a runway surface comprised of 0.91 m wide ground cover cloth laid over dirt. The force plates measured 0.4 m long and 0.6 m wide and were set into a housing box sunk into the center of the runway. The force plates were positioned so that the centers of the plates were 0.52m apart in order to match the approximate distance between footfalls²⁵.



Figure 1.1. Outdoor runway and camera setup.

Two GoPro Hero 5 cameras were positioned perpendicular to the runway on either side of the force plates. The cameras were initially positioned so that approximately 1 m of runway was visible on either side of the force plates. Later on in data collection, the cameras were moved back to increase the field of view to approximately 3 m of runway on either side of the force plates.

For the pulling component of this study, sled dog harnesses were used to harness the dogs to a small sled. A tug line with an elastic element ran between the harness and the sled. A custom in-line force transducer was placed between the tug line and the sled in order to measure the pulling force. The pulling force was adjusted by increasing or decreasing the load on the sled. Because surface conditions changed throughout the study, the frictional force had to be recalibrated prior to each data collection session. In order to calibrate the frictional force, the sled was loaded from 0 kg to 22.7 kg in 2.27 kg increments with an initial 1.13 kg increment, the sled was pulled across the runway at a steady walk, and the force reading from the in-line force transducer for each load was recorded.

Experimental Protocol

There were three treatment conditions with each dog participating in all three treatments in a repeated measures design. In all conditions, the dogs were led across the force plates by a handler with a leash attached to the dog's collar or harness. Water was provided ad libitum and rests were given as needed. The handlers were asked to lead the dogs across the plates at a steady trot. If the dog walked or broke into a gallop, the handler was asked to adjust their speed accordingly. Speeds were

also adjusted in order to match speeds between treatment conditions. Speeds were assessed qualitatively at the time of data collection and then determined quantitatively using video data in postprocessing.

For each condition, trials were collected until 10 steady state trotting trials were collected with a full set of footfalls or until it became clear that the dog would not trot under the treatment conditions. Real time GRF data were monitored using LabChart. For analysis, we selected a cycle of footfalls containing 1 fore GRF followed by simultaneous fore and hind GRFs and ending with one hind GRF. Force data were collected using a 6 s trigger that saved data 3 s before and 3 s after the trigger event. The force data were triggered manually as the dog crossed the plates.

The first condition consisted of an unloaded trotting trial in which the dogs were led across the plates without being harnessed to any load. In the second and third conditions, the dogs were led across the plates while pulling a load. If the dogs would not trot without motivation, they were motivated with food rewards.

Prior to the loading conditions, the dog's weight and standing weight distribution were determined by having the dog stand on the force plates with the forelimbs on one plate and the hindlimbs on the other plate. The weight of the dog was used in combination with the regression of sled load and frictional force to determine the required sled load in the pulling trials. The required sled load for a given frictional force was rounded to the nearest 1.13 kg. For the first and second pulling conditions, the sled load was determined so as to produce a frictional force of 5% and 10% BW respectively.

Pulling behavior was highly variable between dogs. Some dogs would not trot steadily while pulling. In these cases, the load on the sled was reduced. After initial trials, the length of the tugline between the harness and the sled was increased so that the dogs could stop trotting before the sled contacted the force plates. In addition, the weights loading the sled were taped together in order to reduce noise that could startle or distract the dogs. If the dog still did not trot, then the dog was excluded from the study.

This study could be improved by collecting data from the same dogs over multiple data collection sessions. Most dogs were only available for one data collection session. Two dogs were available for three data collection sessions and showed marked improvement by the third session.

Force Data

GRFs were measured using the two previously mentioned custom built force plates. Vertical GRF impulses and peaks were measured. Anterior-posterior GRF impulses and peaks were measured for both propulsive and braking GRFs. GRFs were normalized to BW, and GRF impulses were

normalized to stride time and presented as the mean GRF over the stride. The distribution of vertical, braking, and propulsive GRFs between the forelimbs and the hindlimbs was measured relative to total vertical, braking, and propulsive GRFs respectively. In addition, the individual limb braking-propulsive bias was measured using the absolute value of the braking forces over the sum of the absolute value of the braking forces and the propulsive forces. Resultant fore, hind and total GRF angles were calculated relative to the horizontal. Resultant GRF angles were calculated at 10% intervals over the stride. GRF data for unpaired fore and hind footfalls was collected as well as GRF data from paired footfalls. GRF data from paired footfalls was analyzed separately from unpaired footfalls in order to determine if unpaired footfall data skewed fore-hind GRF distribution measurements. For the pulling trials, pulling forces were collected using the in-line force transducer and were averaged over the stride duration corresponding to the force plate data. Peak pulling forces were recorded.

Force Plates

The two custom built force plates were based off of Heglund, 1981 and Shine, 2016³⁴⁻³⁵. The plates were designed so as to be capable of mediolateral force sensing, however forces in this axis were not measured for this study. Each force plate is composed of a top plate resting on four beams which are mounted to a base plate. The plates measure 60.96 cm by 40.64 cm, with anterior-posterior forces being measured perpendicular to the long axis of the plates.

In order to obtain a light and stiff top plate, a sandwich panel was used. It is important to use a top plate which is both light and stiff in order to obtain a natural frequency which is high enough to be readily distinguished from the signal of interest. Past studies have used aluminum honeycomb sandwich panels in order to obtain these qualities (Heglund, 1981)³⁴. I found that I could obtain a high natural frequency at a much lower cost by using a sandwich panel comprised of 2.54 cm thick end grain balsa with 1.52 mm thick aluminum facing. I used CoreLite BALSASUD paneling for this purpose because it is precoated to reduce epoxy resin absorption. Uncoated end grain balsa can absorb a considerable amount of epoxy which both increases the cost of sandwich construction and increases the end weight of the panel, thereby reducing the natural frequency.

The top plate is supported by two 1.905 cm square aluminum 7075 beams along the anterior and posterior edge of the plate. The top plate is fastened to each beam by six bolts along the middle of the beam. The lateral bolts are placed 8.75 cm medial to either end of the beam, leaving an 8.75 cm wide overhang along the lateral edges of the force plate. The ends of the anterior and posterior beams are supported by two additional beams which lie perpendicular to the uppermost beams and support them at the corners. The upper beams contain a total of 8 spring elements that are instrumented so as

to measure vertical and anterior-posterior forces. The two lower beams contain four spring elements that are instrumented to measure mediolateral forces. The spring elements in the upper beams are placed at the ends of each beam between the top plate bolts and the corner bolts fastening the upper beams to the lower beams. The spring elements in the lower beams are placed at the ends of each beam between the corner bolts and four additional bolts that fasten the lower beams to the base plate.

The beams are composed of aluminum 7075. This material was chosen for its high elastic limit strain. In contrast to Shine, 2016, solid beams were used rather than square tubes³⁶. This decision was made because of the high cost and limited availability of extruded aluminum 7075. One unintended consequence of this, was that the wiring could not be run through the center of the beams. While using solid beams allows for the use of alloys with better mechanical properties, the exposed wiring that results from this design is more easily damaged than the wiring in hollow tube designs.

Each spring element is designed in a binocular double beam design (Figure 1.2). For each spring element, two holes were machined into the beam perpendicular to the axis of the force being measured. A line was then cut between the two holes in order to form a double beam spring element with the strain concentrated at the surface of the beam above and below each machined hole. The primary benefit of the binocular beam design is that the spring element is thickened outside of the area of strain concentration. This results in increased stiffness and a corresponding increase in natural frequency without a reduction in maximum strain³⁶.

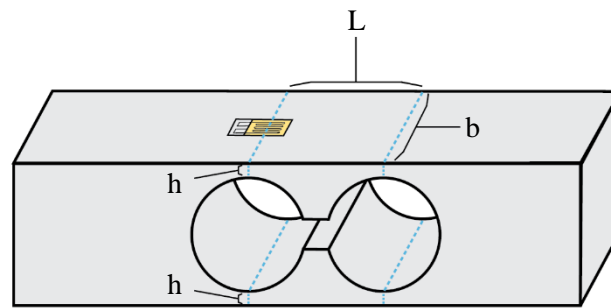


Figure 1.2. Binocular double beam spring element design.

The maximum strain experienced at the point of strain concentration in a connected cantilever beam is given by Eq. 1, where ϵ is strain, P is the maximum load on the beam, L is full length of the beam, E is the elastic modulus of the beam material, b is the width of the beam, and h is the thickness of the beam at the point of strain concentration. This equation can be modified for a double beam design using Eq. 2. For a binocular beam design, L is the length of the beam between the apex of each machined hole (Figure 1.2).

$$\varepsilon = \frac{3PL}{Ebh^2} \quad (1.1)$$

$$\varepsilon = \frac{3PL}{2Ebh^2} \quad (1.2)$$

Beam dimensions for a given force can be calculated by holding P at the desired maximum force and holding ε at the elastic limit strain for the beam material used. When calculating beam dimensions, it is important to consider machining tolerances. Tolerances for beam thickness, h, should be strict as small changes in this dimension can result in large changes in strain. I used a ± 0.5 mm tolerance for the spring element dimensions. I optimized the spring elements for a maximum vertical force of 3000 N and a maximum shear force of 2000 N. In a study of 129 dogs over a wide size range, Voss et al. found mean trotting peak GRFs to be 1.142 BW (95% CI = 0.941, 1.343)³⁷. Taking the upper limit of this CI, peak vertical trotting GRFs for a 50 kg dog can be estimated at 659 N, giving a safety factor of 4.5 for the vertical spring elements. While anterior posterior GRFs during steady state trotting are usually quite low (~ 0.0161 BW)²⁵, they can be considerably higher during active shear force production. Walter and Carrier measured GRFs during rapid acceleration in dogs and found mean peak anterior-posterior forces of 1.34 BW³². Taking this value, peak anterior-posterior GRFs for a 50 kg dog can be estimated at 657 N, giving a safety factor of 3 for the anterior-posterior spring elements. In reality, the maximum anterior-posterior GRFs are likely to be much lower than this even during pulling trials. Taylor 1957 examined the work output of freight sled dogs and found that the maximum instantaneous pulling force during trotting was 642 N for a 9 dog team, or roughly 0.186 BW per dog³⁸. Taking this value, peak anterior-posterior GRFs for a 50 kg dog can be estimated at 91.4 N, giving a safety factor of 21 for the anterior-posterior spring elements.

The vertical spring elements are wired in two Wheatstone bridge formations, one across the anterior spring elements and the other across the posterior spring elements. This allowed for the measurement of the anterior-posterior center of pressure using the ratio of anterior bridge output to posterior bridge output. The total vertical force was measured using the summed output of the anterior and posterior bridges. The anterior-posterior spring elements were wired in one Wheatstone bridge across the entire plate.

The beam assembly is bolted to a base plate comprised of 4 1.9 cm thick MDF boards glued together. A canvas cover is placed over the beam assembly and underneath the top plate in order to provide protection from the environment. The force plates were set in a 95 cm by 66 cm housing box which was sunk into the center of the runway. The force plates were aligned using bolts in the

housing box that fit into holes drilled into the bottom of the base plates. A # cm thick separator ran between the force plates in the housing box.

Output from the force plates was amplified using 6 Micro-Measurements 2210 B Signal Conditioning Amplifiers. The gain for all channels was set at 3300. The analog signal was converted using an AD Instruments Powerlab 16 ADC. Data were collected using LabChart by AD Instruments. Data from the force plates was collected at 1 kHz. Force plate data were filtered in MatLab using a low pass 4th order Butterworth filter. Vertical GRFs acting upwards and horizontal GRFs in the direction of travel were considered positive.

The force plates were initially calibrated using a series of weights placed in the center of the plates from 0 to 22.7 kg in 2.27 kg increments. Subsequent field calibrations were conducted using 0, 2.27, and 11.3 kg. Shear forces were calibrated using an Ametek Chatillon K-DFX-200 digital force gauge. Initial shear force calibrations were conducted in the lab in both compression and tension by using the digital force gauge to push or pull on the edge of the top plate. Pulling calibrations were conducted using a line running from the digital force gauge to a hook. Subsequent field calibrations were conducted in compression only as the housing box obstructed the hook in tension tests. Vertical force and shear force were linearly related with force plate output with an $R^2 > 0.99$ for both plates in both vertical and shear.

In-line Force Transducer

The in-line force transducer used for the pulling trials made use of a strain ring design based off of Almeida, Vaz, Urgueira, and Borges, 2012³⁹. The transducer is composed of an aluminum 6061 ring with an outside diameter of 7.62 cm a width of 2 cm and a wall thickness of 3.175 mm. Two eye bolts are placed facing opposite each other in-line with axis of force. Two strain gauges are placed on each side of the ring perpendicular to the axis of force, with two gages on the outside of the ring measuring compression and two gages on the inside of the ring measuring tension. These four gages are wired in Wheatstone bridge formation.

The maximum strain experienced in a ring in tension is given by Eq. 3, where ϵ is strain, P is the maximum load in tension, r is the ring radius, E is the elastic modulus of the ring material, l is the ring width, and t is the thickness of the ring wall⁴⁰.

$$\epsilon = \frac{1.09Pr}{Elt^2} \quad (1.3)$$

The ring dimensions for a given force can be calculated by holding P at the desired maximum force and holding ϵ at the elastic limit strain for the ring material used. You can then alter the ring width for an aluminum tube of a given radius and wall thickness. The maximum force for my in-line transducer dimensions and material is 1168 N. Given the estimated peak pulling force for a 50 kg dog discussed earlier, this gives a safety factor of 12.8.

The output from the in-line force transducer was amplified using a SparkFun Load Cell Amplifier based off an HX711 IC. The load cell amplifier collected data with a sampling rate of 80 Hz and sent the analog data to an Arduino Mega 2560. The Arduino stored the data on a micro SD card using a SparkFun OpenLog breakout board and an Adafruit DS3231 Precision real time clock. This assembly was housed in a 3D printed box which was mounted to the sled along with a battery pack containing 4 9V batteries. The in-line force transducer was initially calibrated by suspending a series of light weights under 0.5 kg from the force transducer followed by a series of 2.27 kg weights from 2.27 kg to 11.3 kg. Subsequent in-field calibrations were conducted by suspending a series of 2.27 kg weights from 2.27 to 9.07 kg. Part way through data collection an additional 1.13 kg weight was added to the in-field calibration procedure.

Video Data

Video data were used to measure trunk velocity, foot on foot off events, and basic morphometrics. Trunk velocity and foot on foot off events were used to determine steady state trials and to derive contact times, swing times, duty factor, stride duration, stride length. Duty factor was defined for the forelimb and the hindlimb as the mean fore or hindlimb contact time over the stride time. Morphometrics measured from video included height at the withers, height at the hip, back height, and body length. Height at the hip was measured as back height midway between the rump and the most proximal point of the cranial aspect of the hindlimb. In order to account for variability in height at the withers and height at the hip measurements, the length between the withers measurement point and the hip measurement point was measured as well as the length between the withers and the rump. Morphometrics were taken from video of the dogs standing stationary.

Two GoPro Hero 5 cameras were used. The cameras were placed on either side of the force plates, perpendicular to the runway and facing the force plates. Video was recorded at 240 Hz and 720p resolution. Video analysis was done using ProAnalyst (ProAnalyst, Xcitex Inc.). Video data were calibrated in the sagittal plane using the length of the force plate housing box. Trunk velocities were determined by digitizing a point on the head or trunk. The use of privately-owned pets prevented the use of traditional marking methods such as shaving and painting the dogs. In addition, some dogs possessed long coats which made it difficult to observe anatomical landmarks from video data. In

order to overcome these obstacles, points on collars and harnesses were used to track trunk velocity as well as more traditional points such as the nose and the base of the tail. When possible, two or more points were tracked, and the average trunk velocity was taken.

Foot on and foot off events were recorded for 1 complete stride while the dogs were crossing the force plates. The foot on frame was recorded as the first frame in which the foot visibly deformed after making contact with the ground. The foot off frame was recorded as the frame immediately prior to the frame in which the foot can first be seen to leave the ground. In some cases, there was not a clear view of the distal segments of the foot. In these cases, the missing foot on/foot off event was determined by either determining the event timing from the contralateral camera or by observing the deformation of more proximal segments of the foot. The stride was defined from the first forefoot contact to the subsequent contact of the starting foot's contralateral hindlimb. This method of defining the stride was chosen because only two force plates were used, which meant that the starting hindlimb and the ending forelimb were off the plate. The contact of the contralateral hind immediately after the stride served to indicate the approximate timing of the end of the stride and the GRF from this hindlimb was used as an approximation of the hindlimb at the beginning of the stride. Foot on events were used to synchronize both cameras with the force plate data. In order to synchronize the video data with the in-line force transducer, the in-line force transducer was brought in view of the camera and the tugline between the harness and the in-line transducer was pulled 1 or more times.

Steady state was determined following the methods of Shine, 2016³⁵. If the difference between trunk velocity at the beginning of the stride and trunk velocity at the end of the stride differed from the average trunk velocity over the duration of the stride by more than 20%, then the stride was not considered to be steady state and was excluded from the data set.

Statistics

A Student's t-test for correlation was used to test for significant correlation between GRF variables, net shear force, and pulling load. ANCOVA tests were performed to test for significant differences in slope between variables, with either whole animal net shear force or pulling load as the dependent variable and x-velocity as a covariate. Vertical, shear, fore, hind, and net were tested as independent categorical variables. A significance level of $\alpha = 0.05$ was used in all tests.

Results

Morphometrics and Kinematics

Data were collected from 7 dogs for a total of 28 unloaded trotting trials, 35 load 1 trials, and 28 load 2 trials. Initially, it was intended to compare each dog at 5% and 10% BW loads. However, the loading perturbation proved to be highly variable and was therefore analyzed as continuous data. Subject morphometrics are given in Table 2, and stride kinematics are given in Figure 1.3-1.7.

Table 1.2. Morphometrics. All measurements are in cm.

Subject	Withers height	Hip height	Back height	Body length	Withers to hip	Withers to rump
Murphy	67.69	66.08	69.59	82.40	49.85	63.30
Finnegan	66.04	62.56	66.29	79.50	47.83	59.39
Kona	59.22	57.82	59.57	61.52	39.28	48.73
Bear	62.64	58.71	61.47	64.89	37.18	45.68
Hagrid	70.03	66.16	68.80	70.48	40.97	53.93
Lasso	63.49	61.33	63.54	66.72	33.96	45.79
Trooper	70.17	67.27	70.43	73.50	42.28	53.15

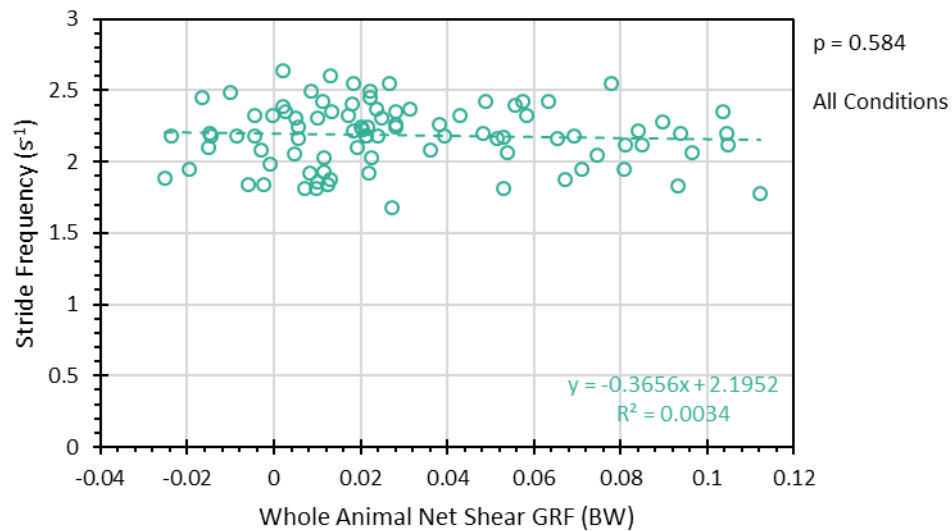


Figure 1.3. Stride frequency vs whole animal net shear over the course of the stride.

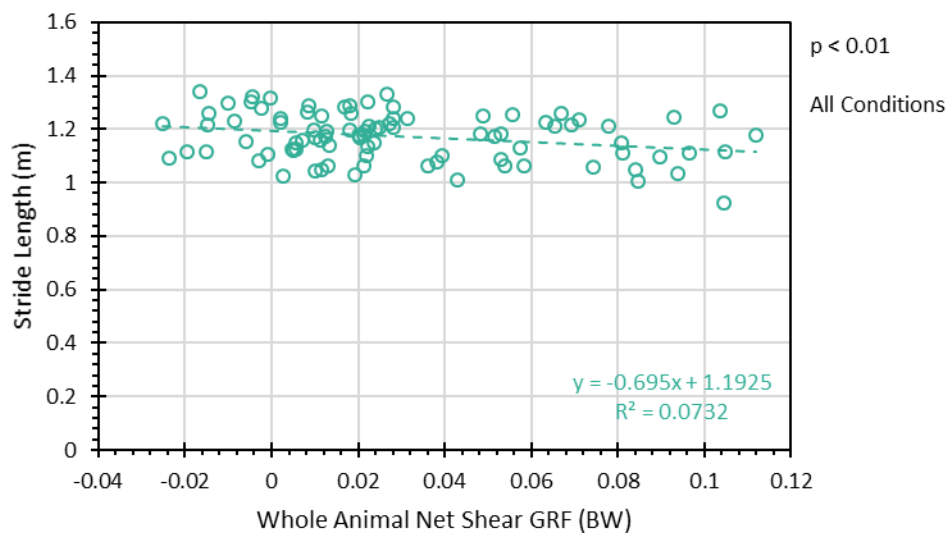


Figure 1.4. Stride length vs whole animal net shear over the course of the stride.

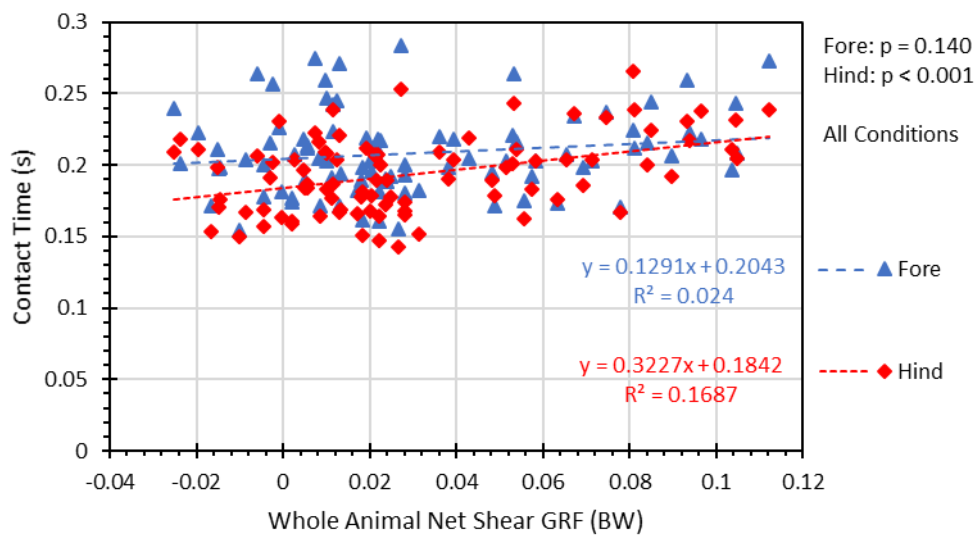


Figure 1.5. Fore and hind contact time vs whole animal net shear over the course of the stride.

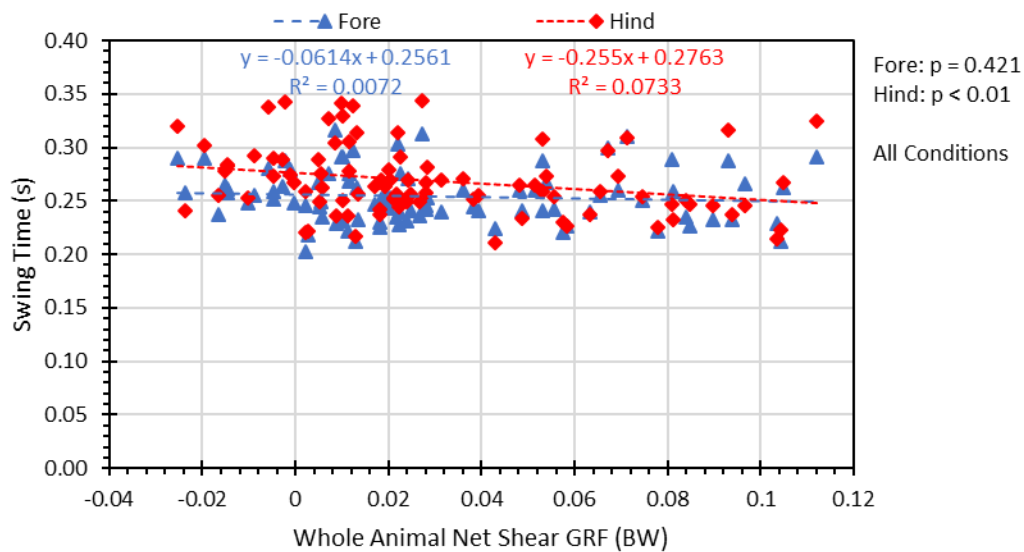


Figure 1.6. Fore and hind swing time vs whole animal net shear over the course of the stride.

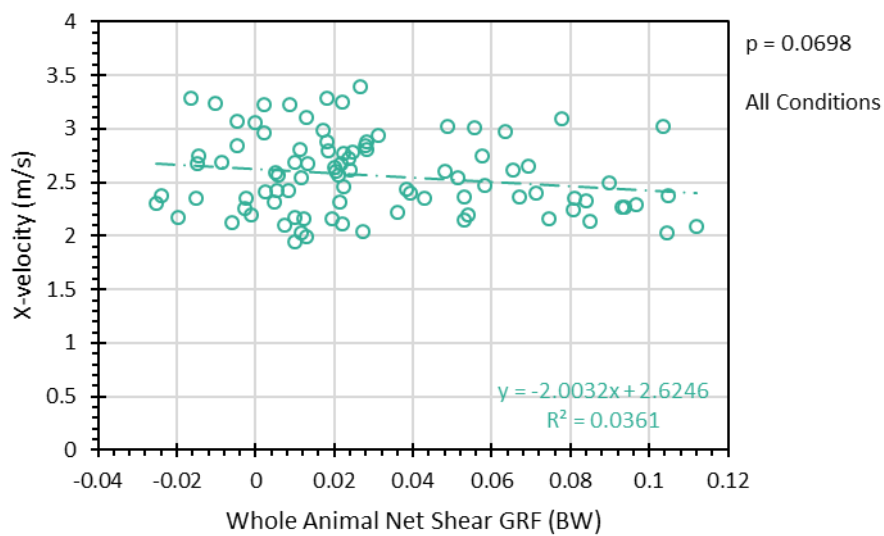


Figure 1.7. Mean x-velocity vs whole animal net shear over the course of the stride.

Ground Reaction Forces

GRFs are shown as the impulse over the stride normalized to body weight and divided by the stride time. This gives the mean GRF over the stride in BW. Limb net GRF refers to the net GRF for an individual limb while net GRF refers to the net GRF for the whole animal.

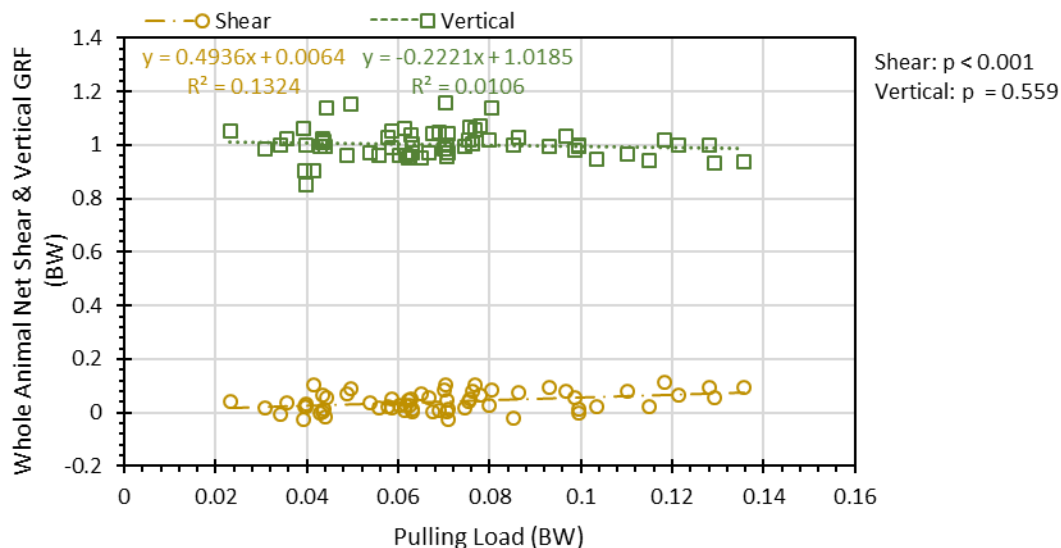


Figure 1.8. Whole animal net shear and vertical GRFs vs mean pulling load over the course of the stride.

As seen in Figure 1.8, mean shear GRF over the stride is positively correlated with pulling load ($r = 0.553$, $p < 0.001$), while mean vertical GRFs are not ($r = 0.0618$, $p = 0.559$). There was a substantial variation in the pulling load (mean standard deviation = 2.98 BW). The baseline magnitude for vertical GRFs was over 100 times greater than that of shear GRFs. This is expected because whole animal net shear GRFs should be 0 under steady state conditions. However, it makes it difficult to graphically compare shifts in vertical and shear GRFs due to the difference in scales. In order to account for this, Figure 1.9 normalizes shear and vertical GRFs by the means of their respective unloaded values.

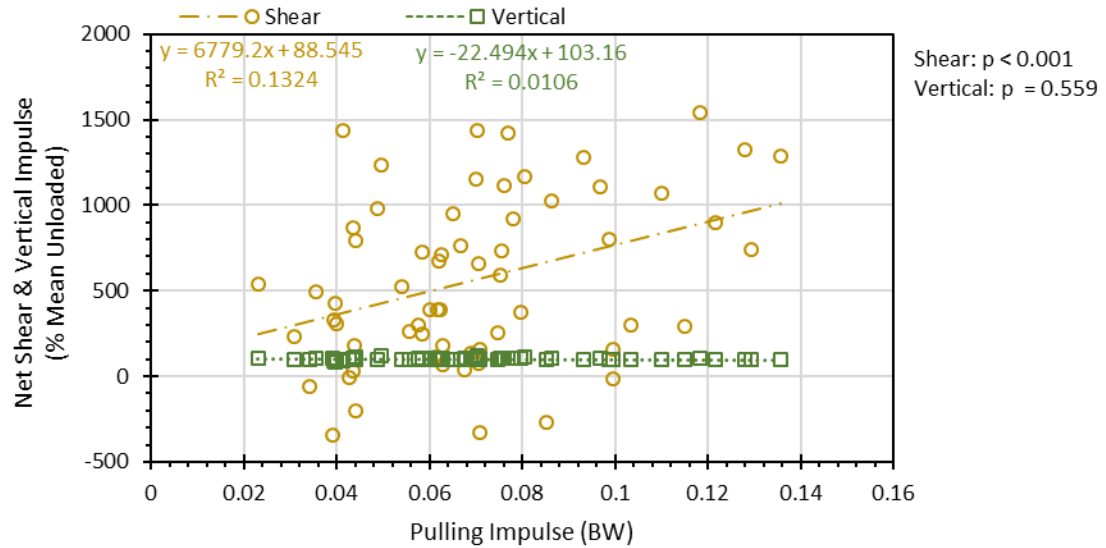


Figure 1.9. Whole animal net shear and vertical GRFs vs. mean pulling load over the course of the stride. Shear and vertical forces are given as % of their unloaded mean.

Whole animal net shear (% mean unloaded) is significantly correlated with pulling load ($r = 0.553$, $p < 0.001$), while vertical (% mean unloaded) is not ($r = 0.0618$, $p = 0.559$). Analysis of covariance with pulling load and mean x-velocity as continuous covariates showed that while GRF component (vertical/shear) is not significant as a main term, there is a significant interaction between pulling load and GRF component ($df = 1$, $F = 0.109$, $p = 0.742$; $df = 1$, $F = 34.3$, $p = 2.30E-8$). No significant effect of x-velocity was found, and there was no significant interaction between x-velocity and GRF component ($df = 1$, 0.126 , $p = 0.723$; $df = 1$, 0.120 , $p = 0.729$).

Shear GRFs

Net shear GRFs were broken into forelimb and hindlimb components. When shown against pulling load, whole animal net shear was shown as Sum.

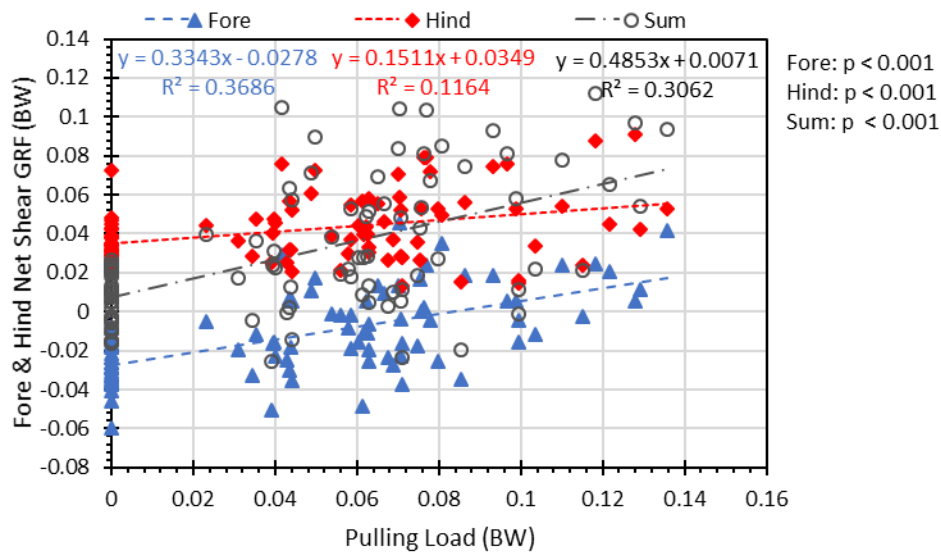


Figure 1.10. Mean forelimb, hindlimb, and whole animal net shear (Sum) GRFs vs. mean pulling load over the course of the stride. All conditions.

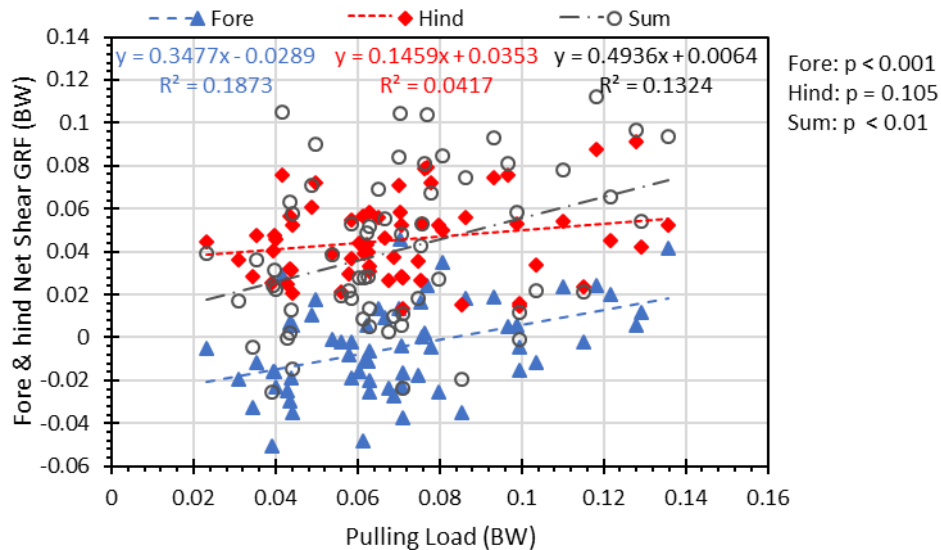


Figure 1.11. Mean forelimb, hindlimb, and whole animal net shear (Sum) GRFs vs. mean pulling load over the course of the stride. Loaded conditions.

Net fore, hind, and whole animal shear GRFs are significantly correlated with pulling load when all conditions are considered (Figure 1.10: Fore: $r = 0.607$, $p < 0.001$; Hind: $r = 0.341$, $p <$

0.001; Sum: $r = 0.553$, $p < 0.001$). However, when only loaded conditions are considered, hind correlation with pulling load becomes nonsignificant (Figure 1.11: $r = 0.204$, $p = 0.105$). Analysis of covariance was conducted for net shear GRFs with Limb (fore, hind) as a categorical covariate and pulling load and mean x-velocity as continuous covariates. Limb was significant as a main term, and there was a significant interaction between pulling load and Limb ($df = 1$, $F = 10.2$, $p = 0.00169$; $df = 1$, $F = 7.49$, $p = 0.00683$). Mean x-velocity did not have a significant effect as a main term, and there was no significant interaction between x-velocity and Limb ($df = 1$, $F = 0.152$, $p = 0.697$; $df = 1$, $F = 0.207$, $p = 0.65$). Significance of covariates was not changed when Sum (summed fore and hind forces) was added in the Limb category.

Evaluating fore and hind net GRFs vs. whole animal net shear GRF results in a significant correlation for the loaded condition subset as well as the whole data set. This trend continues throughout the analysis with most variables showing tighter correlations with whole animal net shear GRF than with pulling load.

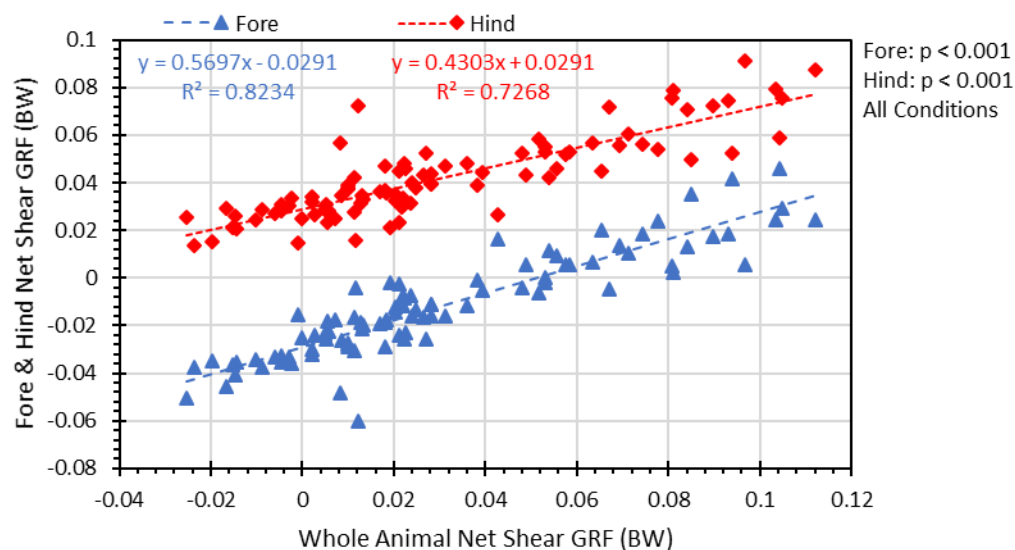


Figure 1.12. Mean forelimb and hindlimb net shear GRFs vs mean whole animal net shear GRF over the course of the stride. All conditions.

Fore and hind net shear GRFs are significantly correlated with whole animal net shear GRF for both the full data set (Figure 1.12) and the loaded trial subset (Full: Fore: $r = 0.907$, $p < 0.001$; Hind: $r = 0.853$, $p < 0.001$; Loaded: Fore: $r = 0.906$, $p < 0.001$; Hind: $r = 0.878$, $p < 0.001$). Analysis of covariance showed that Limb was significant as a main term and also had a significant interaction with whole animal net shear ($df = 1$, $F = 24.3$, $1.91E-6$; $df = 1$, $F = 16.7$, $p = 6.47E-5$). Mean x-

velocity did not have a significant effect either as a main term or as an interaction effect with Limb ($df = 1, F = 0, p = 1$; $df = 1, F = 0.566, p = 0.453$).

The braking component of shear force shifts in response to increased shear loading (Figure 1.13 and 1.14).

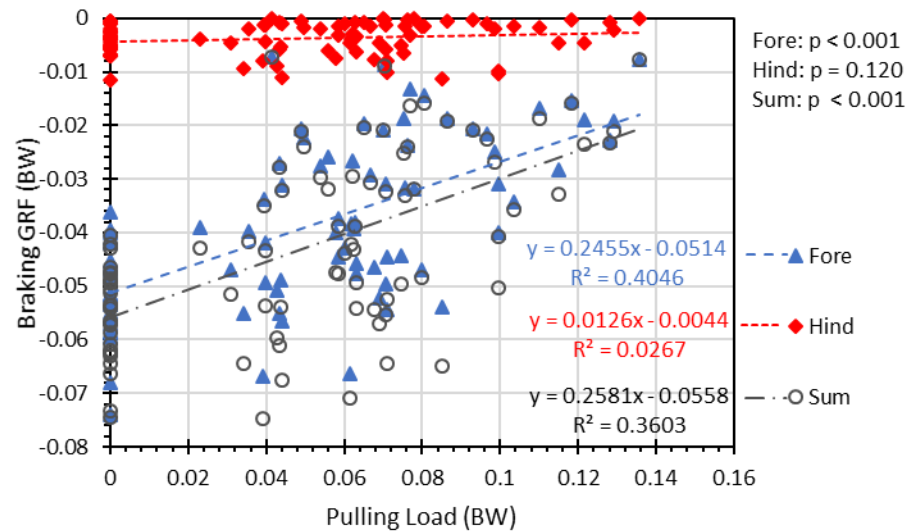


Figure 1.13. Mean forelimb and hindlimb braking GRFs vs mean pulling load over the course of the stride. All conditions.

Fore and the sum of fore and hind braking GRFs are significantly correlated with pulling load; however, hind braking GRFs are not (Figure 1.13: Fore: $r = 0.6361, p < 0.001$; Hind: $r = 0.1634, p = 0.120$; Sum: $r = 0.600, p < 0.001$). Analysis of covariance showed that Limb was significant as a main term and also had a significant interaction with pulling load ($df = 1, F = 14.7, p = 0.00018$; $df = 1, F = 43.6, p = 4.66E-10$). Mean x-velocity did not have a significant effect as either a main term or an interaction term ($df = 1, F = 0.908, p = 0.342$; $df = 1, F = 0.685, p = 0.409$). Limb (Fore, Hind) had a significant effect ($df = 1, F = 622, p = 5.28E-60$). Significance of covariates was not changed when Sum was added in the Limb category.

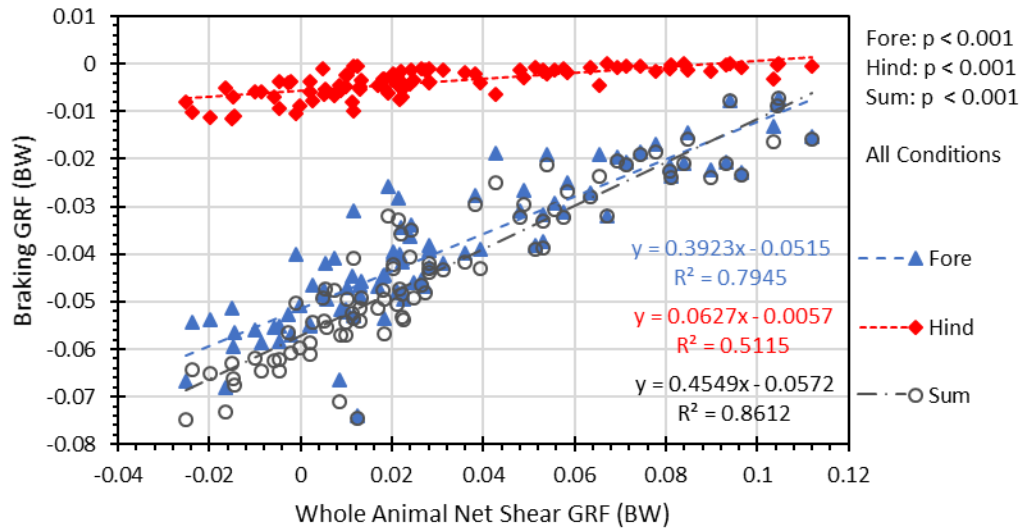


Figure 1.14. Mean forelimb and hindlimb braking GRFs vs mean whole animal net shear GRF over the course of the stride. All conditions.

When braking GRFs are plotted against whole animal net shear GRF, you can see that forelimb, hindlimb, and the sum of fore and hind braking GRFs are all significantly correlated with whole animal net shear GRF (Figure 1.14: Fore: $r = 0.891$, $p < 0.001$; Hind: $r = 0.715$, $p < 0.001$; Sum: $r = 0.928$, $p < 0.001$). Analysis of covariance showed that Limb had a significant effect as both a main term and an interaction term with whole animal net shear ($df = 1$, $F = 38.6$, $p = 3.64E-9$; $df = 1$, $F = 211$, $p = 7.74E-32$). However, x-velocity was also significant as both a main term and an interaction term with whole animal net shear ($df = 1$, $F = 5.43$, $p = 0.0210$; $df = 1$, $F = 3.97$, $p = 0.0479$). Significance of covariates was not changed when Sum was added in the Limb category. When Sum was added to the limb category, the interaction term between x-velocity and Limb became nonsignificant ($df = 2$, $F = 2.18$, $p = 0.115$).

The propulsive components of shear force also shift in response to increased shear loading (Figure 1.15 and 1.16)

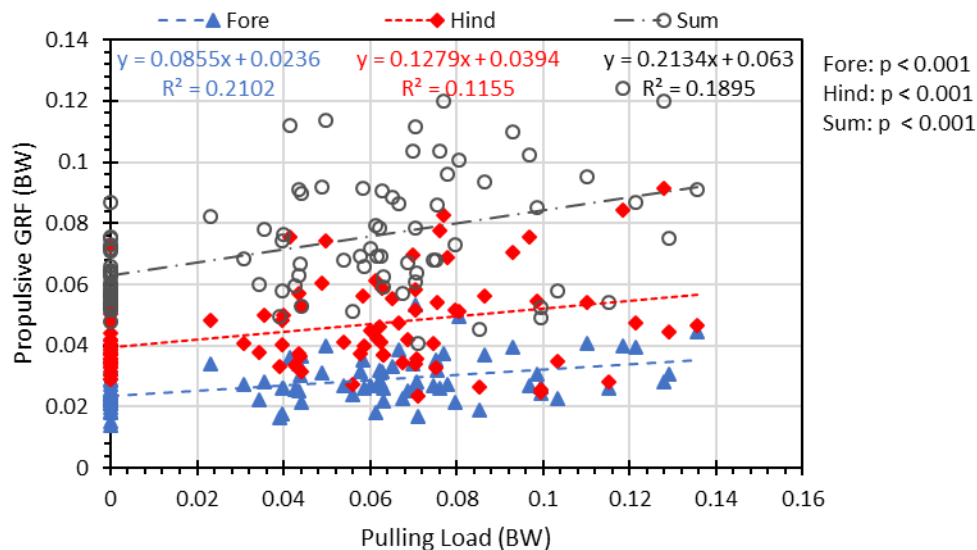


Figure 1.15. Mean forelimb and hindlimb propulsive GRFs vs mean pulling load over the course of the stride. All conditions.

When all conditions are analyzed, fore, hind, and the sum of fore and hind propulsive GRFs are all significantly correlated with pulling load (Figure 1.15: Fore: $r = 0.459$, $p < 0.001$; Hind: $r = 0.340$, $p < 0.001$; Sum: $r = 0.435$, $p < 0.001$). However, when the unloaded trials are excluded, hind and Sum correlations become nonsignificant (Unloaded: Fore: $r = 0.262$, $p < 0.05$; Hind: $r = 0.178$, $p = 0.160$; Sum: $r = 0.234$, $p = 0.0628$). Analysis of covariance showed that Limb was not significant as either a main term or as an interaction term with pulling load ($df = 1$, $F = 3.66$, $p = 0.0575$; $df = 1$, $F = 0.596$, $p = 0.441$). X-velocity was not significant either as a main term or as an interaction term with Limb ($df = 1$, $F = 0.0126$, $p = 0.911$; $df = 1$, $F = 0.500$, $p = 0.480$). When Sum was added in the Limb category, Limb became significant as a main term ($df = 1$, $F = 3.57$, $p = 0.0297$).

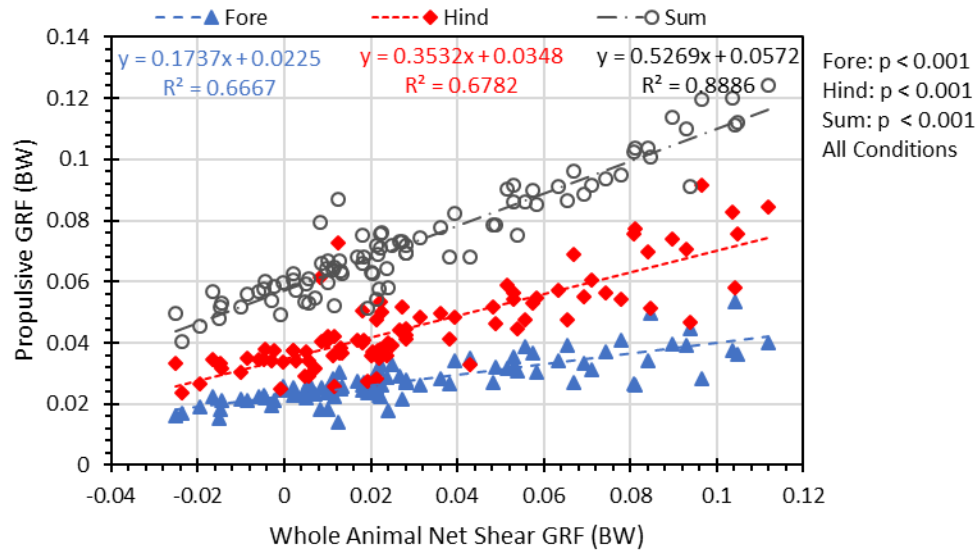


Figure 1.16. Mean forelimb and hindlimb propulsive GRFs vs mean whole animal net shear GRFs over the course of the stride. All conditions.

Fore, hind, and the sum of fore and hind propulsive GRFs are all significantly correlated with whole animal net shear GRF (Figure: 1.16: Fore: $r = 0.817$, $p < 0.001$; Hind: $r = 0.824$, $p < 0.001$; Sum: $r = 0.943$, $p < 0.001$). In contrast to pulling load, analysis of covariance with whole animal net shear showed that Limb had a significant effect as both a main term and an interaction term with whole animal net shear ($df = 1$, $F = 4.27$, $p = 0.0403$; $df = 1$, $F = 36.3$, $p = 9.87E-9$). X-velocity did not have a significant effect as either a main term or as an interaction term ($df = 1$, $F = 2.88$, $p = 0.0916$; $df = 1$, $F = 0.175$, $p = 0.676$). However, when Sum was added in the Limb category, x-velocity became significant as a main term, although it was still nonsignificant as an interaction term with Limb ($df = 1$, $F = 7.98$, $p = 0.00509$; $df = 1$, $F = 1.96$, $p = 0.621$).

Although the distribution of shear forces within the fore and hindlimbs changes, the overall distribution of propulsive and braking forces between the limbs did not change to a statistically significant degree. Figure 1.17 and 1.18 show the change in distribution of shear forces within the limbs while Figure 1.19 and 1.20 show the change in distribution between the limbs.

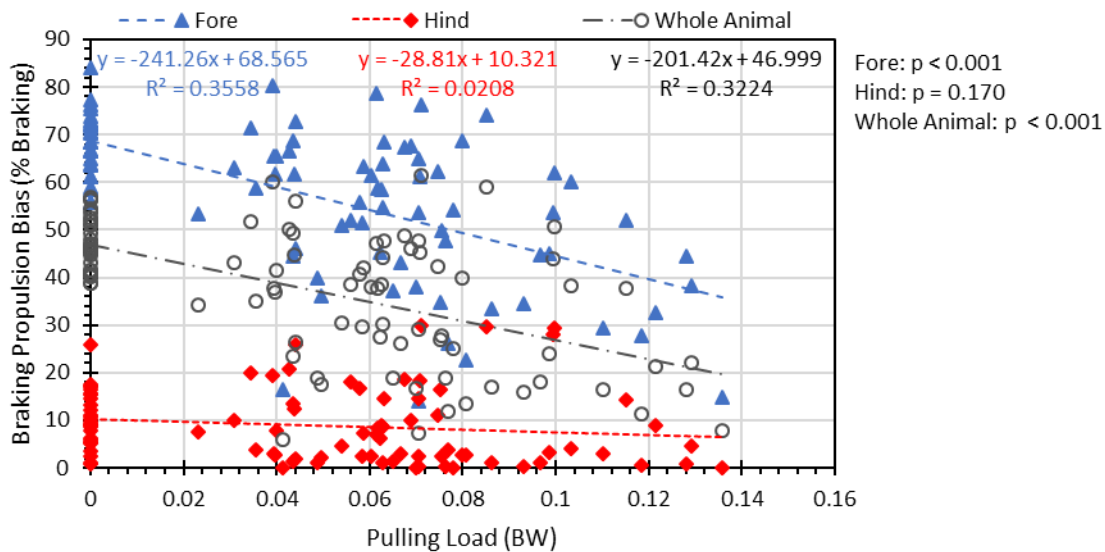


Figure 1.17. Braking-propulsion bias vs mean pulling load over the course of the stride. All conditions.

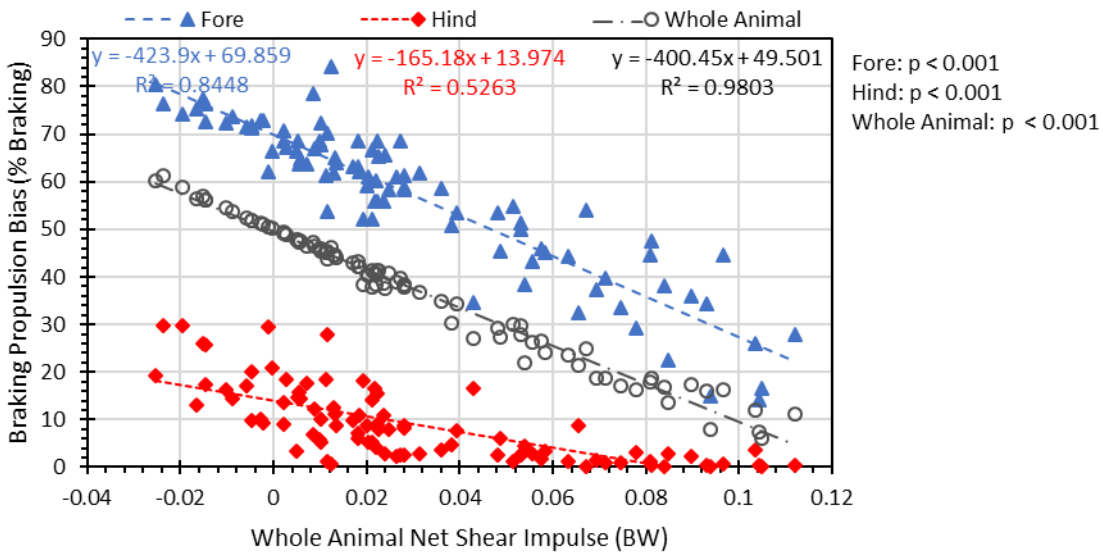


Figure 1.18. Braking-propulsion bias vs whole animal net shear over the course of the stride. All conditions.

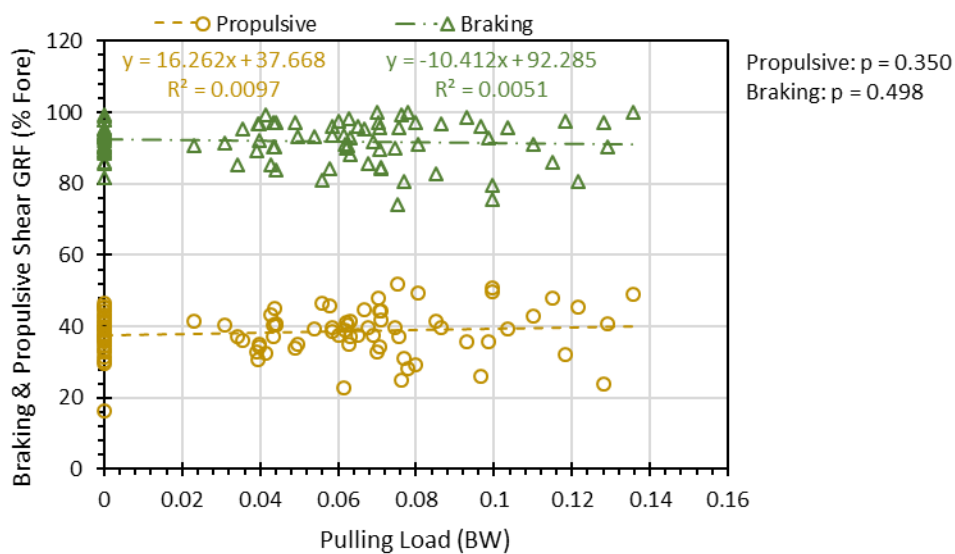


Figure 1.19. Percent of propulsive and braking forces provided by the forelimbs vs pulling load over the course of the stride. Propulsive and braking forces not provided by the forelimbs are provided by the hindlimbs. All conditions.

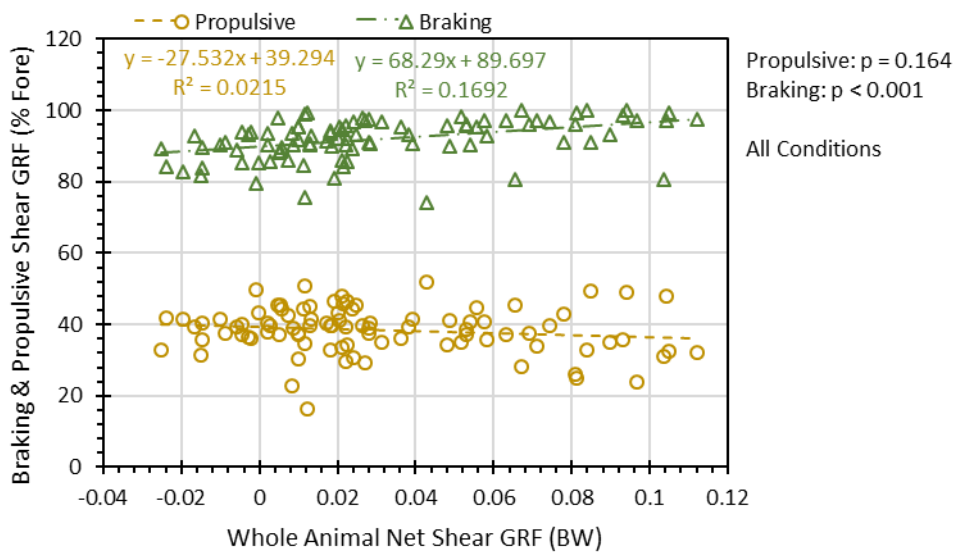


Figure 1.20. Percent of propulsive and braking forces provided by the forelimbs vs whole animal net shear over the course of the stride. Propulsive and braking forces not provided by the forelimbs are provided by the hindlimbs. All conditions.

Fore and whole animal braking-propulsion bias are significantly correlated with whole animal pulling load, while hind braking-propulsion bias is not (Figure 1.17; Fore: $r = -0.596$, $p < 0.001$; Hind: $r = -0.144$, $p = 0.170$; Whole Animal: $r = -0.568$, $p < 0.001$). Fore, hind, and whole animal braking-propulsion bias are all significantly correlated with whole animal net shear GRF (Figure 1.18; Fore: $r = -0.919$, $p < 0.001$; Hind: $r = -0.725$, $p < 0.001$; Whole Animal: $r = -0.99$, $p < 0.001$). Analysis of covariance showed that Limb was significant as a main term and as an interaction term with both pulling load and whole animal net shear. (pulling load: $df = 1$, $F = 20.5$, $p = 1.09E-5$; $df = 1$, $F = 24.8$, $1.48E-6$; whole animal net shear: $df = 1$, $F = 56.9$, $p = 2.42E-12$; $df = 1$, $F = 95.2$, $p = 3.08E-18$). Mean x-velocity did not have a significant effect as a main term or as an interaction effect in either analysis (pulling load: $df = 1$, $F = 0.0608$, $p = 0.806$; $df = 1$, $F = 0.0104$, $p = 0.919$; whole animal net shear: $df = 1$, $F = 0.436$, $p = 0.510$; $df = 1$, $F = 0.939$, $p = 0.334$). Adding Whole Animal to in the Limb category did not affect the significance of any of the covariates.

In contrast to within limb braking-propulsion bias, the only significant correlation to the between limb distribution of braking and propulsive forces (% Fore) was the correlation of Braking % Fore to whole animal net shear GRF (Figure 1.20; $r = 0.411$, $p < 0.001$). Shear component (braking/propulsive) did become significant as a main term when considered with pulling load as a dependent variable ($df = 1$, $F = 77.9$, $p = 1.09E-15$). However, shear component was not significant as an interaction effect with pulling load ($df = 1$, $F = 2.13$, $p = 0.146$). Shear component became significant as both a main term and as an interaction effect when considered with whole animal net shear ($df = 1$, $F = 62.7$, $p = 2.71E-13$; $df = 1$, $F = 13.4$, $p = 0.00033$). X-velocity had no significant effect as either a main term or an interaction term with either pulling load or whole animal net shear (pulling load: $df = 1$, $F = 0.581$, $p = 0.447$; $df = 1$, $F = 1.62$, $p = 0.205$; whole animal net shear: $df = 1.96$, $p = 0.163$; $df = 1$, $F = 0.0483$, $p = 0.826$). Adding whole animal net shear as a category in shear component resulted in shear component no longer being significant as a main effect in the pulling load analysis.

Vertical GRFs

Vertical GRFs decrease at the forelimb and increase at the hindlimb with pulling load and whole animal net shear GRF (Figure 1.21 and 1.22). Fore and hind vertical GRFs are significantly correlated with pulling load (Figure: 1.21: Fore: $r = -0.494$, $p < 0.001$; Hind: $r = 0.588$, $p < 0.001$). Fore and hind vertical GRFs are also significantly correlated with whole animal net shear (Figure 1.22: Fore: $r = -0.392$, $p < 0.001$; Hind: $r = 0.645$, $p < 0.001$). Summed fore and hind vertical GRFs are not significantly correlated with pulling load or whole animal net shear GRFs (respectively, $r = 0.0618$, $p = 0.559$; $r = 0.184$, $p = 0.0796$).

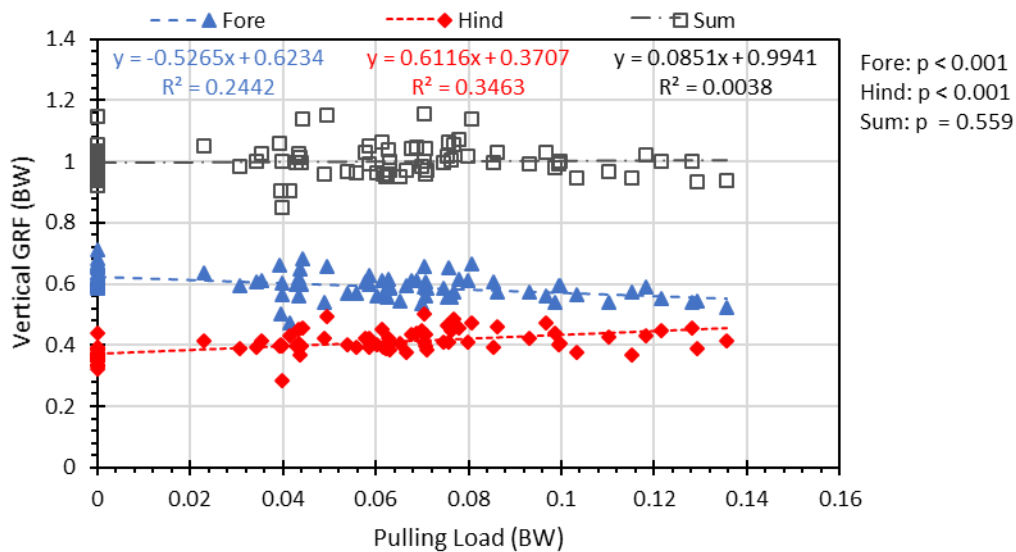


Figure 1.21. Mean fore, hind, and summed fore and hind vertical GRFs vs. mean pulling load over the stride.

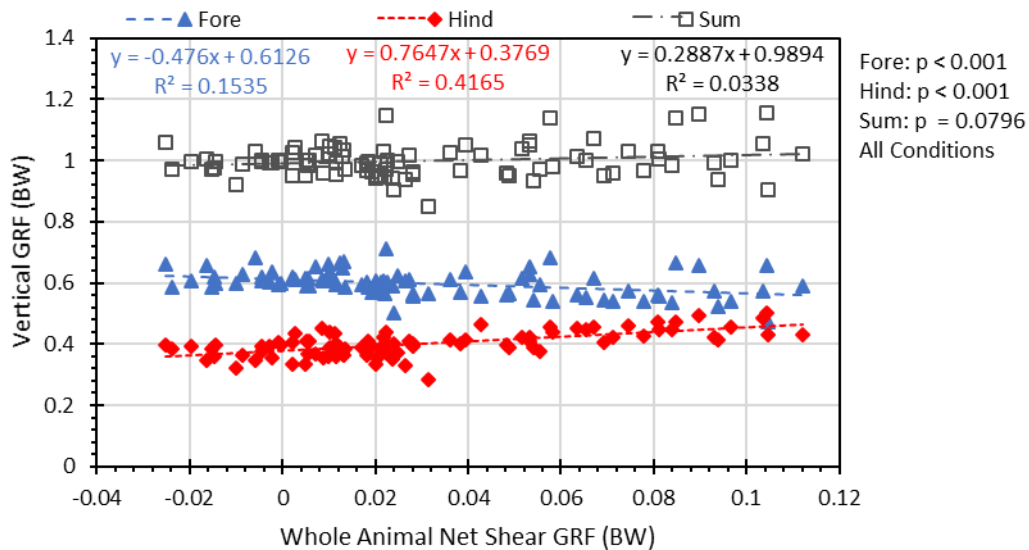


Figure 1.22. Mean fore, hind, and summed fore and hind vertical GRFs vs. mean whole animal net shear GRF over the stride.

Analysis of covariance with mean vertical GRF showed that Limb was significant as a main term and as an interaction term with both pulling load and whole animal net shear. (pulling load: $df = 1$, $F = 49.4$, $p = 4.51E-11$; $df = 1$, $F = 73.9$, $p = 4.51E-15$; whole animal net shear: $df = 1$, $F = 35.0$, $p = 1.71E-8$; $df = 1$, $F = 64.7$, $p = 1.26E-13$). However, mean x-velocity had a significant effect as a main term in the pulling load analysis ($df = 1$, $F = 7.26$, $p = 0.00774$). Adding Sum to in the Limb category resulted in x-velocity having a significant effect as a main term in the whole animal net shear analysis as well ($df = 1$, $F = 4.78$, $p = 0.0297$).

Vertical GRF % Fore is significantly correlated with both pulling load and whole animal net shear GRF (Figure 1.23: pulling load: $r = -0.713$, $p < 0.001$; Figure 1.24: whole animal net shear: $r = -0.699$, $p < 0.001$). Analysis of covariance found no significant main term effect of pulling load or whole animal net shear on vertical GRF % Fore (respectively, $df = 1$, $F = 0.307$, $p = 0.581$; $df = 1$, $F = 0.0296$, $p = 0.864$). X-velocity was also found to have no significant effect as either a main term or as an interaction term with pulling load or whole animal net shear (pulling load: $df = 1$, $F = 1.59$, $p = 0.211$; $df = 1$, $F = 3.80$, $p = 0.0544$; whole animal net shear: $df = 1$, $F = 1.76$, $p = 0.188$; $df = 1$, $F = 1.13$, $p = 0.291$). When analysis of covariance was run with x-velocity as a covariate but without the interaction effects, both pulling load and whole animal net shear were found to have highly significant main term effects on vertical GRF % fore (respectively, $df = 1$, $F = 84.3$, $p = 1.73E-14$; $df = 1$, $F = 78.6$, $p = 7.73E-14$).

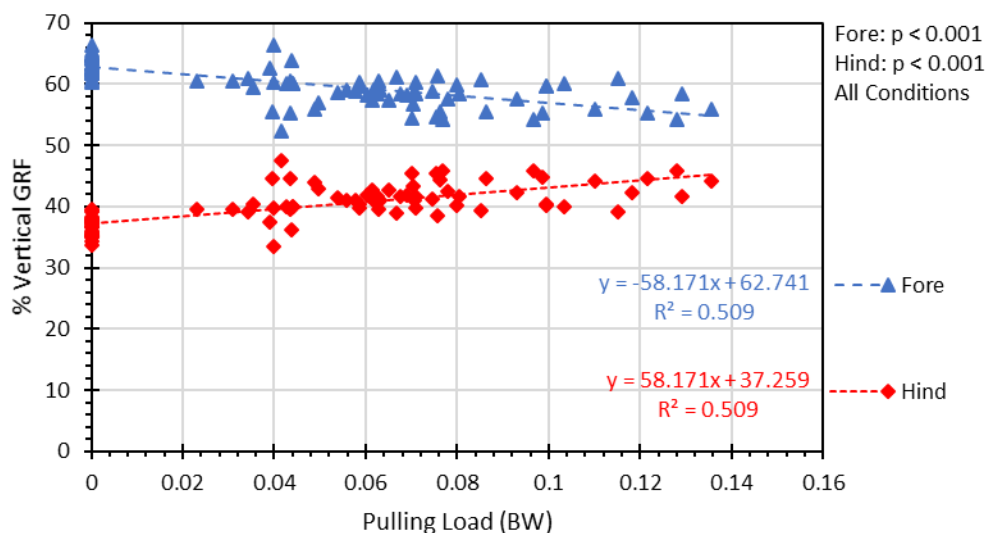


Figure 1.23. % vertical GRF provided by the fore and hindlimbs vs mean pulling load over the stride.

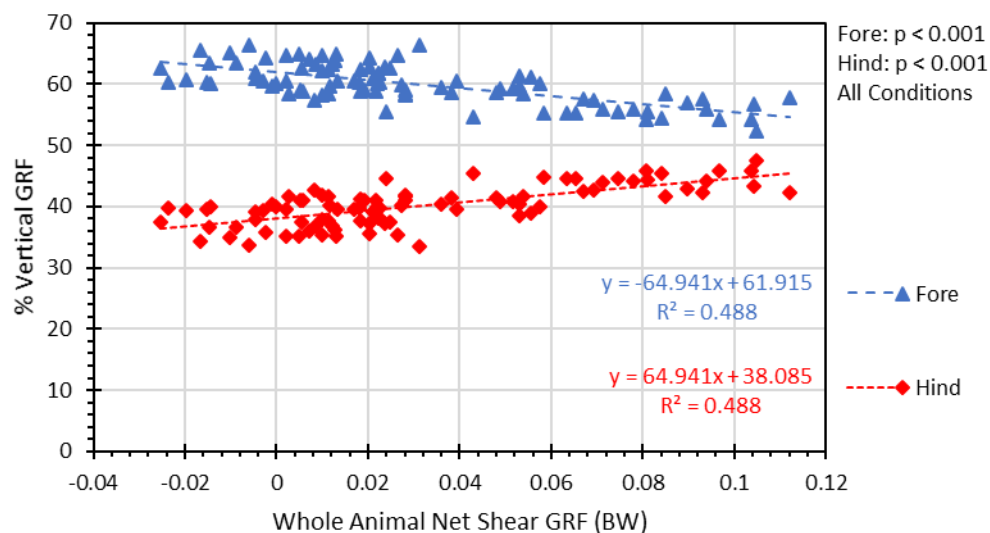


Figure 1.24. % vertical GRF provided by the fore and hindlimbs vs mean whole animal net shear GRF over the stride.

As vertical GRFs shift from the forelimb to the hindlimb, additional vertical GRFs at the hindlimb are produced by increasing duty factor while maintaining or decreasing peak GRF magnitude (Figure 1.25 – 1.28).

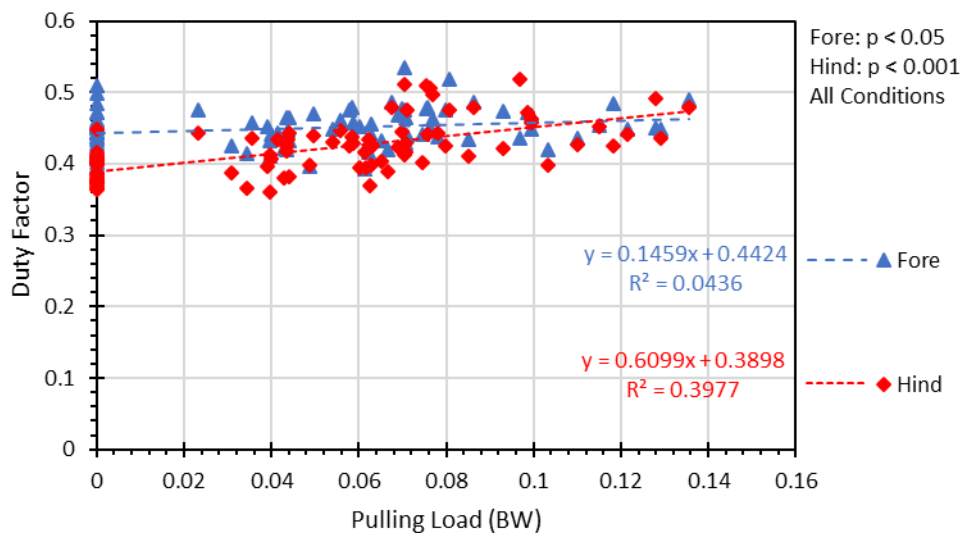


Figure 1.25. Duty factor at the forelimb and hindlimb vs mean pulling load over the stride. Duty factor was defined as the mean fore or hindlimb contact time over stride time.

Fore and hind duty factors are significantly correlated with pulling load (Figure 1.25: Fore: $r = 0.209$, $p < 0.05$; Hind: $r = 0.631$, $p < 0.001$). Analysis of covariance showed that Limb has a significant effect as a main term and as an interaction term with pulling load ($df = 1$, $F = 11.9$, $p = 0.0007$; $df = 1$, $F = 26.1$, $p = 8.53E-7$). However, mean x-velocity covaried significantly with duty factor ($df = 1$, $F = 28.1$, $p = 3.43E-7$).

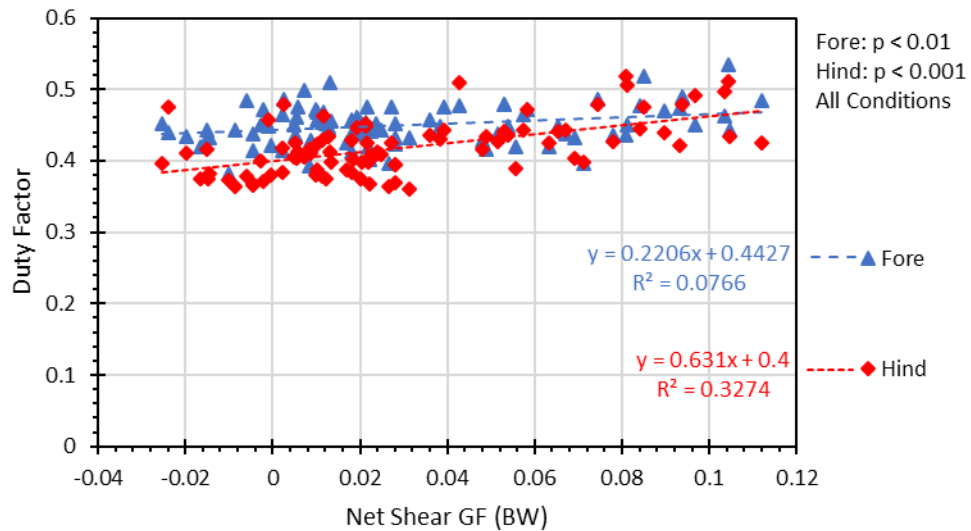


Figure 1.26. Duty factor at the forelimb and hindlimb vs mean whole animal net shear GRF over the stride. Duty factor was defined as the mean fore or hindlimb contact time over stride time.

Fore and hind duty factors are significantly correlated with whole animal net shear GRF (Figure 1.26: Fore: $r = 0.277$, $p < 0.01$; Hind: $r = 0.572$, $p < 0.001$). Analysis of covariance showed that Limb has a significant effect as a main term and as an interaction term with pulling load ($df = 1$, $F = 6.13$, $p = 0.0143$; $df = 1$, $F = 14.5$, $p = 0.00019$). However, mean x-velocity covaried significantly with duty factor ($df = 1$, $F = 28.5$, $p = 2.93E-7$).

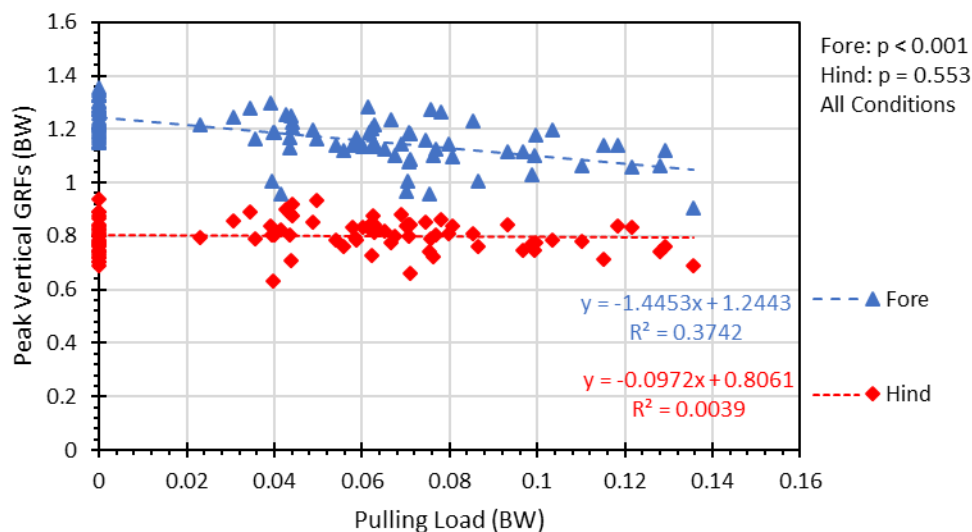


Figure 1.27. Peak vertical GRFs at the forelimb and hindlimb vs mean pulling load over the stride.

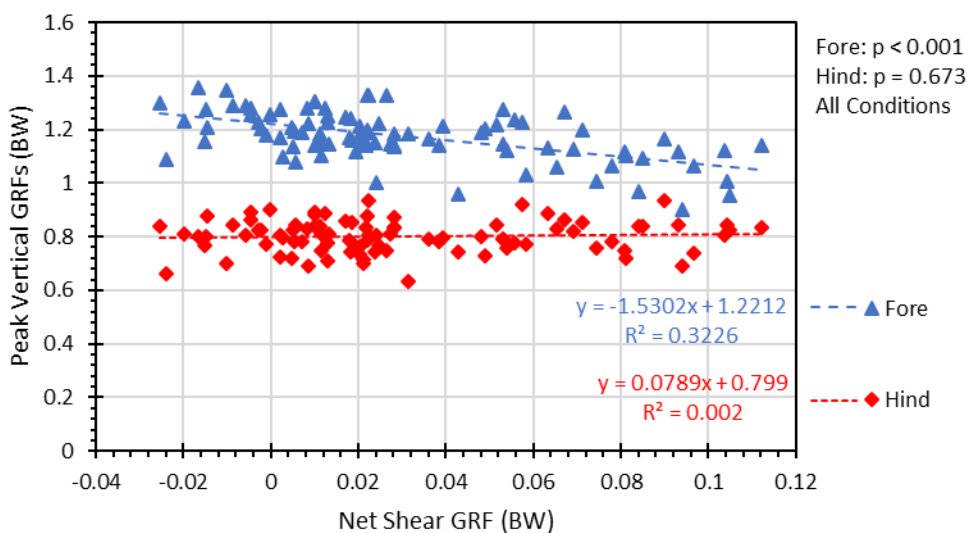


Figure 1.28. Peak vertical GRFs at the forelimb and hindlimb vs mean whole animal net shear GRF over the stride.

Fore peak vertical GRFs are significantly correlated with pulling load and whole animal net shear GRF (respectively, $r = -0.612$, $p < 0.001$; $r = 0.568$, $p < 0.001$). Hind peak vertical GRFs are not significantly correlated with pulling load or whole animal net shear GRF (respectively, $r = -0.0627$, $p = 0.553$; $r = 0.0446$, $p = 0.673$). Analysis of covariance showed that Limb had a significant effect

main term effect as well as a significant interaction with pulling load ($df = 1, F = 15.3, p = 0.00013$; $df = 1, F = 20.9, p = 8.94E-6$). Limb also had a significant main term effect and interaction term for whole animal net shear ($df = 1, F = 12.4, p = 0.00054$; $df = 1, F = 24.5, p = 1.78E-6$). However, there was a significant interaction term between x-velocity and Limb for the whole animal net shear analysis ($df = 1, F = 4.17, p = 0.0428$).

Resultant GRFs

As propulsive forces increase with increasing shear load, the net resultant angle shifts forward for both the forelimbs and the hindlimbs (Figure 1.29 and 1.30).

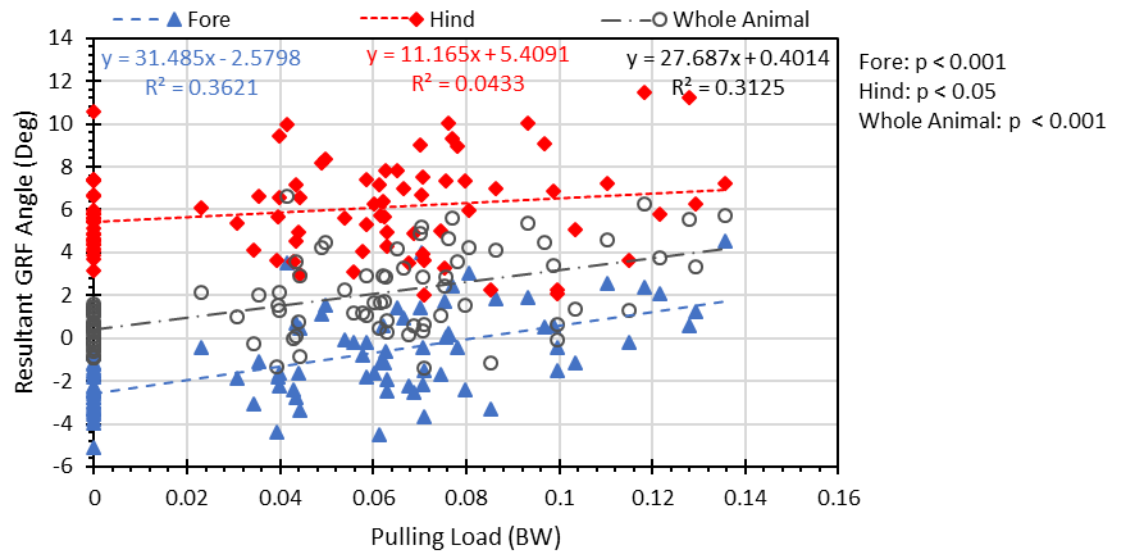


Figure 1.29. Fore, hind, and whole animal resultant GRF angle vs mean pulling load over the stride.

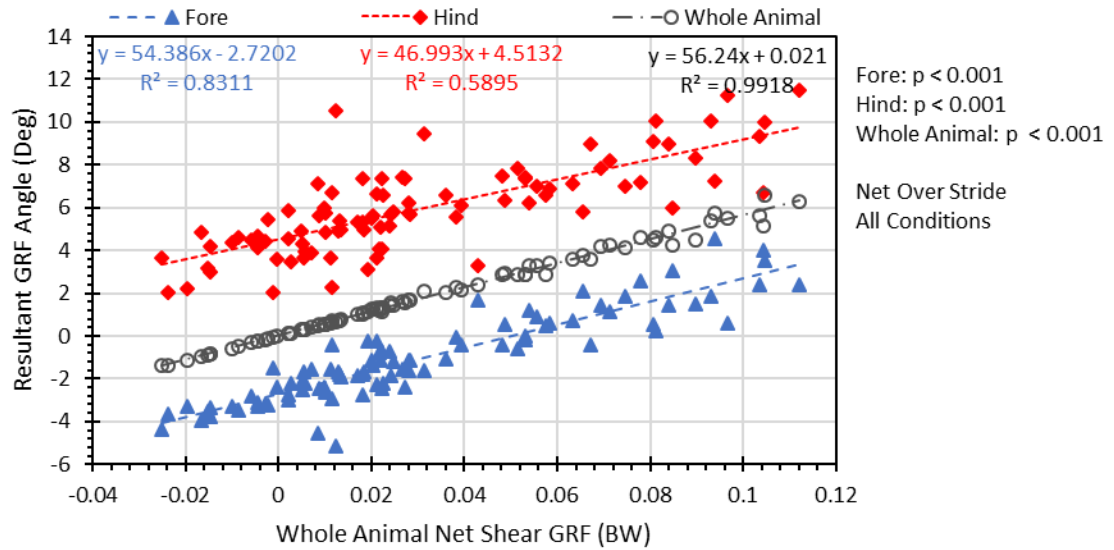


Figure 1.30. Fore, hind, and whole animal resultant GRF angle vs mean whole animal net shear GRF over the stride.

Fore, hind, and whole animal resultant GRF angle were significantly correlated with pulling load (Figure: 1.29: Fore: $r = 0.602$, $p < 0.001$; Hind: $r = 0.208$, $p < 0.05$; Whole Animal: $r = 0.559$, $p < 0.001$). Analysis of covariance with pulling load found a significant main term effect for Limb but did not find a significant interaction term between Limb and pulling load ($df = 1$, $F = 8.08$, $p = 0.005$; $df = 1$, $F = 0.793$, $p = 0.374$). Fore, hind, and whole animal resultant GRF angle were also correlated with whole animal net shear GRF (Figure 1.30: Fore: $r = 0.912$, $p < 0.001$; Hind: $r = 0.768$, $p < 0.001$; Whole Animal: $r = 0.996$, $p < 0.001$). Analysis of covariance found a significant main term effect for Limb as well as a significant interaction term between Limb and whole animal net shear ($df = 1$, $F = 11.1$, $p = 0.00106$; $df = 1$, $F = 8.58$, $p = 0.00385$). Adding Whole Animal to in the Limb category did not affect the significance of any of the covariates.

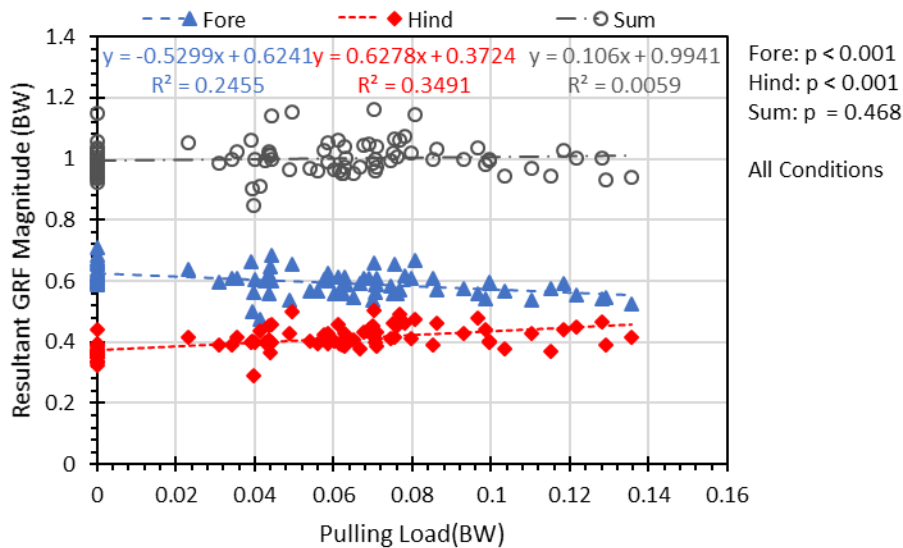


Figure 1.31. Fore, hind, and summed fore and hind resultant GRF magnitude vs mean pulling load over the stride.

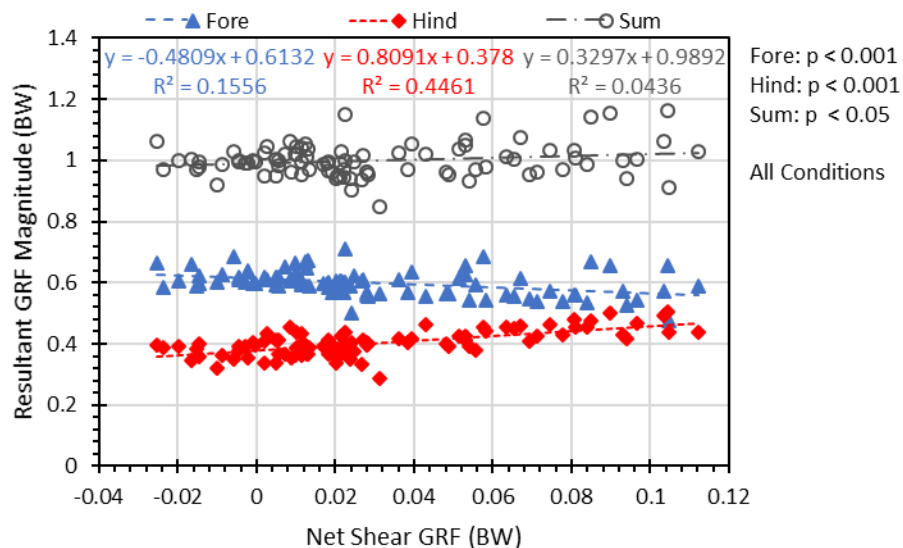


Figure 1.32. Fore, hind, and summed fore and hind resultant GRF magnitude vs mean whole animal net shear GRF over the stride.

Fore and hind resultant GRF magnitude were significantly correlated with pulling load and whole animal net shear (Pulling load: Fore: $r = -0.496$, $p < 0.001$; Hind: $r = 0.591$, $p < 0.001$; Whole animal net shear: Fore: $r = -0.394$, $p < 0.001$; Hind: $r = 0.668$, $p < 0.001$). However, summed fore and

hind resultant GRF magnitude was only significantly correlated with whole animal net shear ($r = 0.209$, $p < 0.05$).

Discussion

Objective 1

The first objective of this thesis was to determine whether vertical and shear force decoupling between the forelimbs and the hindlimbs is maintained during active shear force production during submaximal locomotion. Two hypotheses were made with regards to this objective. First, it was hypothesized that vertical and shear force production by the forelimbs would not increase during pulling trials (Hypothesis 1a). This would be consistent with the division of labor between the fore and hindlimbs with vertical force production at the forelimbs being decoupled from shear force production at the hindlimbs. A second related hypothesis was that shear force production by the hindlimbs would increase proportionally to the load in the pulling trials consistent with the division of labor between the fore and hindlimbs with shear force production provided by the hindlimbs (Hypothesis 1b). The results of this study clearly showed that complete vertical and shear force decoupling between the forelimbs and the hindlimbs does not exist during submaximal shear force production. However, looking at the results more closely shows that both hypotheses 1a and 1b are partially supported.

Shear Force Production

As whole animal net shear GRFs increase, net shear force production increases across both the forelimbs and the hindlimbs, with the rate of increase at the forelimbs being significantly greater than that at the hindlimbs (Figure 1.10-1.12). However, while net shear force production by the forelimbs increases in response to shear loading, this is primarily due to decreased braking (Figure 1.13-1.14). Under unloaded conditions, the forelimbs produce a mean $92.3 \pm 1.52\%$ of braking forces. The production of braking force by the forelimbs decreases from a mean of -0.051 ± 0.0032 BW over the course of the stride under unloaded conditions, to a mean of -0.034 ± 0.0036 BW under loaded conditions. At the highest whole animal net shear, forelimb braking across the stride dropped to a mere -0.0154 BW; however, this still represents $97.5 \pm 1.17\%$ of all braking forces. Braking by the hindlimbs also decreases significantly with whole animal net shear; however, as hindlimb braking is very low to begin with, the effect of this is less noticeable than at the forelimbs.

The production of propulsive forces is more evenly distributed than the production of braking forces. The forelimbs produce $37.9 \pm 0.023\%$ of propulsive forces under unloaded conditions. As

whole animal net shear increases, propulsive force production increases at both the forelimbs and the hindlimbs (Figure 1.15-1.16). However, the rate of increase at the hindlimbs is slightly more than twice the rate of increase at the forelimbs. At the highest whole animal net shear, the forelimbs produce $32.15 \pm 1.32\%$ of propulsive forces.

These changes in GRF production result in a shift in braking-propulsion bias within the limbs (Figure 1.17-1.18). Following the linear trend in Figure 1.18, the hindlimbs start out propulsive biased, with 14% of hindlimb shear forces being braking at 0 BW whole animal net shear. As net shear increases, the hindlimbs become progressively more propulsion biased until nearly all shear forces being produced by the hindlimbs are propulsive. In contrast, the forelimbs start out heavily braking biased with 70% of forelimb shear forces being braking at 0 BW whole animal net shear. The forelimbs shift to being propulsive biased at 0.047 BW net shear, with braking-propulsion bias declining to 27.5% braking at 0.1 BW net shear.

Despite the shift in braking-propulsion bias within the limbs, the overall fore/aft distribution of braking and propulsive forces changes very little with whole animal net shear (Figure 1.19-1.20). Although, the forelimbs shift from being braking biased to being propulsion biased, the coinciding increase in hindlimb propulsive forces results in the overall fore/aft distribution of propulsive forces becoming more heavily biased towards the hindlimbs with increasing whole animal net shear. This shift was only significant for braking % fore vs whole animal net shear force; however, the gradual slope that is observed is positive for braking and negative for propulsion. In other words, as shear loading increases, propulsive shear force production becomes more biased towards the hindlimbs while braking becomes more biased towards the forelimbs. Thus, while the forelimbs are not completely decoupled from shear force production at the hindlimbs, the forelimbs are partially decoupled from shear force production in that shear force production is heavily biased towards the hindlimbs and this bias is maintained during active shear force production.

Vertical Force Production

The observed shifts in shear force production with whole animal net shear are accompanied by shifts in vertical force production. However, unlike the shift in propulsive and braking force production, vertical force production becomes more evenly distributed between the forelimbs and the hindlimbs as shear force production increases (Figure 1.21-1.24). Vertical force production by the hindlimbs increases, while vertical force production by the forelimbs decreases with whole animal net shear. The significance of this correlation depends on the limb in question and the analysis used. With a t-test for correlation, mean forelimb and hindlimb vertical GRFs over the stride were significantly correlated with both pulling load and whole animal net shear GRF. Analysis of covariance showed a

significant interaction between Limb and whole animal net shear; however, when Sum was added in the Limb category, x-velocity became a significant covariate. When looking at the percent of vertical GRFs provided by the forelimb, the significance of the relationship with whole animal net shear depended on whether the analysis of covariance included interaction terms between whole animal net shear and mean x-velocity. In both cases, x-velocity was insignificant as a main term; however, adding interaction terms between whole animal net shear and x-velocity resulted in the whole animal net shear becoming insignificant as both a main term and as an interaction term. The results of Lee's acceleration studies support the observed relationship between shear force production and the fore/aft distribution of vertical force production²⁵. However, in this study this relationship was nonsignificant in some analyses due to x-velocity being a significant covariate.

The increase in mean vertical GRFs over the stride by the hindlimbs was accomplished by increasing duty factor at the hindlimbs while holding peak vertical GRFs constant (Figure 1.25-1.28). This was accompanied by a significant decrease in peak vertical GRFs at the forelimbs and a slight, but significant increase in duty factor at the forelimbs.

These results complicate the question of vertical and shear force decoupling. While shear force production is heavily biased towards the hindlimbs, and this bias is maintained during active shear force production, the forward bias of vertical force production shifts towards the hindlimbs with increased shear force production. Lee explained this shift in vertical force production as a means for countering a tipping moment about the center of mass that is generated during active shear force production²⁵. While moments generated by resultant GRFs were not measured in this study, the observed shift in the distribution of vertical force production is consistent with Lee's conclusions.

Objective 2

The second objective of this thesis was to determine whether the function of the forelimbs as struts and the hindlimbs as levers is maintained during active shear force production in submaximal locomotion. Two related hypotheses addressed this objective. The first hypothesis was that the direction of the resultant ground reaction force at the forelimbs would be maintained during loaded trials consistent with continued strut type action at the forelimbs as opposed to lever type action in response to the shear load (Hypothesis 2a). The second hypothesis was that the direction of the resultant ground reaction force at the hindlimbs would shift forward during loaded trials consistent with shear forces being produced by the hindlimbs via a lever type action (Hypothesis 2b).

Hypothesis 2a was not supported. As the limbs become increasingly propulsion biased, the resultant GRF angle shifts forward at both the forelimbs and the hindlimbs (Figure 1.29-1.30). The angle of the forelimb resultant GRF shifts forward significantly more rapidly than that of the

hindlimb. However, the forelimb mean resultant GRF angle starts out negative and does not become positive until approximately 0.05 BW whole animal net shear. Hypothesis 2b is supported in that the resultant GRF angle at the hindlimb has a significant positive correlation with whole animal net shear.

Resultant GRF Angle

While the resultant GRF angle remaining constant would certainly indicate the absence of lever type retraction, the fact that the resultant GRF shifts forward does not necessarily confirm lever type retraction. Active contraction about the proximal limb joint, such as is seen in lever type retraction, results in the resultant GRF shifting forward; however, the resultant GRF can shift forward under the strut model of locomotion so long as the resultant GRF passes through the joint center. In order for the resultant GRF to shift forward while still passing through the joint center, it is necessary to increase limb retraction angle so that the foot is displaced behind the joint center. Following the linear regression of resultant GRF angle vs whole animal net shear as seen in Figure 1.30, the maximum observed GRF angle occurs at about 0.115 BW net shear. At 0.115 BW net shear, the resultant GRF angle is 3.53 deg forward of vertical for the forelimbs and 9.12 deg forward of vertical for the hindlimbs. Using an average hip height of 0.47 m as reported for 5 Labradors²⁵, this would require a foot displacement behind the joint center of 0.029 meters for the forelimb and 0.082 meters for the hindlimb. While foot displacement was not measured, a qualitative analysis of the data does not support the existence of foot displacements as large as 0.08 m.

Resultant GRF Magnitude

As can be seen by comparing Figure 1.31-1.32 and Figure 1.21-1.22, the relative magnitudes of shear and vertical GRFs results in the resultant GRF magnitudes largely following vertical GRF magnitudes. However, it is interesting to note that the resultant GRF magnitude at the forelimbs decreases significantly with whole animal net shear. Furthermore, if you take the steady state resultant GRF magnitude at the forelimbs, and then use the angle of retraction at the forelimbs at 0.115 BW whole animal net shear, it becomes apparent that the observed increase in net shear force at the forelimbs with increasing whole animal net shear could be accomplished by changing forelimb angle without increasing forelimb resultant GRF magnitude.

Relation to Other Studies

The results of this study closely mirror the results of other studies on active shear force production in dogs. As mentioned earlier, Carrier et al. 2006 is the first in a series of 5 papers that investigate EMG activity of the extrinsic appendicular muscles under various loading conditions^{22,23}.

This series of studies includes pulling as a load perturbation and provides insight into pulling activity that cannot be addressed from a GRF perspective. They found that 4 of the primary retractor muscles of the hip, including the cranial portion of the biceps femoris, superficial gluteus, medial gluteus, and semimembranosus⁴⁰ were active early in stance during steady state trotting. In contrast, they found no activity during stance in the major extrinsic forelimb retractor muscles they studied²³ When they applied a pulling load, they observed increased activity in the hindlimb retractor muscles⁴⁰ as well as initiation of activity in the extrinsic forelimb retractor muscles, including the pectoralis profundus and latissimus dorsi²³ These findings are consistent with the ground reaction forces in this study, and strongly suggest that the observed increase in forelimb propulsion was due at least in part to active retraction about the proximal limb joint. Carrier et al. also looked at forelimb and hindlimb EMG activity during incline trotting and found similar activity, with an increase in hindlimb retractor activity accompanied by the recruitment of previously silent proximal forelimb retractors^{23,40}.

Lee, 2011 examined GRFs during incline trotting in dogs and found a similar response to increased inclines as was observed for pulling in this study. Trotting uphill resulted in increased duty factor at the hindlimbs and a redistribution of vertical GRFs to the hindlimbs, with vertical GRF % fore going from approximately 65% to 53% fore²⁴. Lee also found that the resultant GRF angle shifts forwards at both the fore and hindlimbs during incline trotting and that the hindlimbs exerted approximately 59% of the total propulsive impulse²⁴. In a separate study on steady state level trotting, Lee found the propulsion bias at the hindlimbs to be more than 3 times the braking bias at the forelimbs³⁰.

Yet another study by Lee examines the distribution of force across the forelimbs and the hindlimbs in accelerating dogs²⁵. In this study, Lee found that the distribution of vertical force production is shifted towards the hindlimbs as dogs accelerate²⁵. Lee explains this shift in vertical force production as a means for balancing the tipping moment generated about the hip²⁵. In addition, Lee notes that the distribution of net shear force production shifts towards the forelimbs with acceleration²⁵. Both of these results are observed in this study.

Conclusions

Overall, the results of this study show that shear force production during submaximal locomotion is achieved in largely the same manner whether you are talking about acceleration, inclines, or pulling. In all three cases, shear force production occurs by increasing net shear force production across both the forelimbs and the hindlimbs while shifting vertical force production towards the hindlimbs. This basic pattern persists across acceleration, inclines, and pulling despite timing differences and limb posture constraints that are associated with each loading regime.

Although the results of this study did not differ from past studies on submaximal shear force production, there is one result which should be noted. Namely, that there is a significant and functionally important difference between the within limb distribution of shear forces, the fore/aft distribution of net shear forces, and the fore/aft distribution of braking and propulsive forces. Since many studies focus on the distribution of vertical forces between the forelimbs and the hindlimbs, it is common to report the distribution of shear forces in terms of the net shear force without breaking this down into its braking and propulsive components. Looking at the shift in the distribution of net shear forces gives the false impression that the distribution of propulsive force production shifts towards the forelimbs with increasing acceleration. If you look at the within limb braking-propulsion bias, this impression is maintained because the reduction of braking by the forelimbs results in a drastic shift in braking-propulsion bias. However, the fact that a larger proportion of the shear forces being produced by the forelimbs are propulsive does not indicate that there is a corresponding shift at the level of the whole animal. In fact, as shear force production increases the fore/aft distribution of propulsive force production moves in the opposite direction of the fore/aft distribution of net shear force production. The distribution of propulsive force production becomes more biased towards the hindlimbs even as the distribution of net shear force production shifts toward the forelimbs.

This last point has an important bearing on the hypothesis of vertical and shear force decoupling that I mentioned at the beginning of this thesis. It is true that the forelimbs are recruited during active shear force production. However, the overall distribution of propulsive force production remains heavily biased towards the hindlimbs. Furthermore, even though the forelimbs are involved in shear force production, they also experience a reduction in resultant GRF magnitude due to the observed shift in vertical force production. This shift in vertical force production results in the further coupling of vertical and shear force production at the hindlimbs, but it reduces the load on the forelimbs. Considering that the forelimbs still carry more than 50% of the weight during acceleration, vertical and shear force decoupling at the forelimbs may still be functionally important even though it is not complete.

Limitations

Subject Limitations

The use of privately owned dogs resulted in a number of limitations. While this allowed for the recruitment of new subjects over an extended period of time, the limited availability of individual subjects meant that there was little opportunity for animals to become habituated to the experimental setup. Future studies might be improved by collecting data over the course of several days in order to allow time for the dogs to become habituated. This could be taken further by limiting subjects to sled

dogs. Dogs were recruited without regard to pulling experience. By limiting subjects to sled dogs, it may be possible to obtain a higher success rate for the pulling trials. With this being said, it is important to note that previous training might interfere with some aspects of the experimental setup. For instance, many sled dog enthusiasts in the lower 48 participate in relatively short races. Because of this, sled dogs are often trained to run at high speeds. This could make it difficult to obtain steady trotting trials at matched speeds for both the light and heavy loading conditions.

In addition to the limited availability of subjects, using privately owned dogs also limited the methods that could be used, especially with regards to marking joint centers. While joint centers could be marked fairly easily for short haired dogs, long haired dogs would require shaving in order to enable traditional marking methods. Future work could benefit by exploring marking methods that do not require shaving. One possible solution would be to use markers that could be clipped to the fur; however, it would be difficult to achieve a marker that is stable without sacrificing visibility due to overlapping fur.

Equipment Limitations

The force plates and in-line force transducer used in this study were custom made. While this was far more economical than using commercially available equipment, some aspects of the design could be improved. For instance, the base was constructed of 4 1.9 cm thick MDF boards glued together. Varying environmental conditions throughout the course of the study eventually led to swelling in the base material. Due to this, sand had to be applied to the force plate housing prior to each data collection section in order to level the force plates. This introduced an additional source of error in the data. Another limitation was that mediolateral forces were not collected. Considering the limited availability of GRF data for pulling trials, it could be valuable to collect mediolateral GRFs despite their usually being negligible for trotting dogs.

Another limitation concerns the in-line force transducer. Since the in-line force transducer was mounted to the sled, it required a light and portable amplifier. In order to achieve these design specifications, a Sparkfun Load Cell Amplifier was used which incorporated an HX711 IC. This limited the sampling frequency to a maximum of 80 Hz. Because of this, pulling data were limited to the average pulling force as opposed to instantaneous pulling force.

Methodological Limitations

There are also several limitations which result directly from the use of pulling as a load perturbation. Although pulling avoids some of the confounding variables seen in incline and acceleration studies, it has a few unique confounding variables of its own. One of these is the point of

load application. The harnesses used in this study are designed to distribute force against the chest, sternum, and shoulders. Depending on the dog and the angle of pull, the exact relationship of the pulling force to the dog's center of mass may change. If the pulling force travels above or below the center of mass, then this will create a moment about the center of mass. Beyond this, even if the pulling force does travel through the center of mass, if the pulling angle is not horizontal, then there will be a vertical component as well as a shear component to the pulling load. In order to reduce this, the point of attachment on the sled was adjusted so that the tugline was as close to horizontal as possible. However, it is likely that all pulling forces in this study contain some moments about the center of mass as well as a minor vertical component.

Further, it must also be acknowledged that pulling does not provide a continuous load perturbation. Due to the discontinuous nature of legged locomotion, pulling involves a series of tugs. Furthermore, the coefficient of friction varies with surface conditions, making it difficult to maintain a constant pulling load. I used the average pulling force in order to quantify this discontinuous shear load. However, future studies could benefit by looking at the effect of instantaneous shear loads on GRFs.

Speed must be more tightly controlled in order to obtain reliable pulling loads. I defined steady state as any trials where the velocity at the beginning of the stride differs from the velocity at the end of the stride by less than 20%. However, given my average stride time, a non-countered negative accelerating force of 10% BW would result in a change of velocity of -0.45 m/s; this is only 17% of my average x-velocity across all trials. Because of this problem, many of the dogs were effectively countering a load that was considerably less than the intended load. This being said, the result was is still a data set which consists of dogs applying forces which would normally being associated with acceleration without the accompanying positive acceleration. The problem is that many of the dogs were applying low propulsive forces while allowing the load to decelerate them. This led to a high degree of variability in the pulling data and a considerable amount of scatter in the correlation of pulling load with whole animal net shear GRF.

Related to the variability in x-velocity, were some significant covariance with x-velocity throughout the data. X-velocity was a significant covariate in the analysis of covariance of hind and fore peak vertical GRF vs whole animal net shear GRF. X-velocity was also a significant covariate in all duty factor analysis of covariance tests. X-velocity was a significant covariate in the analysis of covariance of fore, hind, and net vertical GRF vs pulling load. X-velocity was a significant covariate with fore and hind shear braking vs. whole animal net shear, although x-velocity was not a significant covariate when net was added to the Limb category.

Literature Cited

- 1) Sharp, C.N.C. (2012). Animal athletes: a performance review. *Veterinary Record* 171(4), 87-94.
<http://dx.doi.org/10.1136/vr.e4966>
- 2) Hubel, T. Y., Myatt, J. P., Jordan, N. R., Dewhirst, O. P., McNutt, J. W., & Wilson, A. M. (2016). Energy cost and return for hunting in African wild dogs and cheetahs. *Nature Communications*, 7, 11034. doi:10.1038/ncomms11034
- 3) Taylor, C., Schmidt-Nielsen, K., Dmiel, R., & Fedak, M. (1971). Effect of hyperthermia on heat balance during running in the African hunting dog. *American Journal of Physiology-Legacy Content*, 220(3), 823-827. doi:10.1152/ajplegacy.1971.220.3.823
- 4) Mech, D.L. & Cluff, D.H. (2011). Movements of wolves at the northern extreme of the species' range, including during four months of darkness. *PLoS One* 6(10):e25328.
<https://doi.org/10.1371/journal.pone.0025328>
- 5) Tarroux, A., Berteaux, D., & Bêty, J. (2010). Northern nomads: ability for extensive movements in adult arctic foxes. *Polar Biology* 33(8), 1021-1026. <https://doi.org/10.1007/s00300-010-0780-5>
- 6) Loftus, J. P., Yazwinski, M., Milizio, J. G., & Wakshlag, J. J. (2014). Energy requirements for racing endurance sled dogs. *Journal of Nutritional Science*, 3, e34.
<http://doi.org/10.1017/jns.2014.31>
- 7) Bryce, C. M., & Williams, T. M. (2016). Comparative locomotor costs of domestic dogs reveal energetic economy of wolf-like breeds. *The Journal of Experimental Biology*, 220(2), 312-321. doi:10.1242/jeb.144188
- 8) Poole, D. C., & Erickson, H. H. (2011). Highly Athletic Terrestrial Mammals: Horses and Dogs. *Comprehensive Physiology*, 1(1), 1-37. doi:10.1002/cphy.c091001
- 9) Miller, B. F., Ehrlicher, S. E., Drake, J. C., Peelor, F. F., Biela, L. M., Pratt-Phillips, S., . . . Hamilton, K. L. (2015). Assessment of protein synthesis in highly aerobic canine species at the onset and during exercise training. *Journal of Applied Physiology*, 118(7), 811-817. doi:10.1152/jappphysiol.00982.2014
- 10) Snow, D. H. (1985). The horse and dog, elite athletes—why and how? *Proceedings of the Nutrition Society*, 44(02), 267-272. doi:10.1079/pns19850046

- 11) Stepien, R. L., Hinchcliff, K. W., Constable, P. D., & Olson, J. (1998). Effect of endurance training on cardiac morphology in Alaskan sled dogs. *Journal of Applied Physiology*, 85(4), 1368-1375. doi:10.1152/jappl.1998.85.4.1368
- 12) Banse, H. E., Sides, R. H., Ruby, B. C., & Bayly, W. M. (2007). Effects of endurance training on VO₂max and submaximal blood lactate concentrations of untrained sled dogs. *Equine and Comparative Exercise Physiology*, 4(02), 89-94. doi:10.1017/s1478061507811455
- 13) Miller, B., Hamilton, K., Boushel, R., Williamson, K., Laner, V., Gnaiger, E., & Davis, M. (2017). Mitochondrial respiration in highly aerobic canines in the non-raced state and after a 1600-km sled dog race. *Plos One*, 12(4). doi:10.1371/journal.pone.0174874
- 14) Alexander, R. M. (2002). Tendon elasticity and muscle function. *Comparative Biochemistry and Physiology Part A: Molecular & Integrative Physiology*, 133(4), 1001-1011. doi:10.1016/s1095-6433(02)00143-5
- 15) Bryce, C. M., & Williams, T. M. (2016). Comparative locomotor costs of domestic dogs reveal energetic economy of wolf-like breeds. *The Journal of Experimental Biology*, 220(2), 312-321. doi:10.1242/jeb.144188
- 16) Goldenberg, F., Glanzl, M., Henschel, J. R., Funk, S. M., & Millesi, E. (2008). Gait choice in desert-living black-backed jackals. *Journal of Zoology*, 275(2), 124-129. doi:10.1111/j.1469-7998.2008.00417.x
- 17) Cavagna, G. A., Heglund, N. C., & Taylor, C. R. (1977). Mechanical work in terrestrial locomotion: Two basic mechanisms for minimizing energy expenditure. *American Journal of Physiology-Regulatory, Integrative and Comparative Physiology*, 233(5). doi:10.1152/ajpregu.1977.233.5.r243
- 18) Cavagna, G. A., Heglund, N. C., & Taylor, C. R. (1977). Mechanical work in terrestrial locomotion: Two basic mechanisms for minimizing energy expenditure. *American Journal of Physiology-Regulatory, Integrative and Comparative Physiology*, 233(5). doi:10.1152/ajpregu.1977.233.5.r243
- 19) Lee, D. V., Bertram, J. E., Anttonen, J. T., Ros, I. G., Harris, S. L., & Biewener, A. A. (2011). A collisional perspective on quadrupedal gait dynamics. *Journal of The Royal Society Interface*, 8(63), 1480-1486. doi:10.1098/rsif.2011.0019

- 20) Alexander, R. M. (2002). Tendon elasticity and muscle function. *Comparative Biochemistry and Physiology Part A: Molecular & Integrative Physiology*, 133(4), 1001-1011.
doi:10.1016/s1095-6433(02)00143-5
- 21) Usherwood, J. R., & Wilson, A. M. (2005). No force limit on greyhound sprint speed. *Nature*, 438(7069), 753-754. doi:10.1038/438753a
- 22) Carrier, D. R. (2006). Locomotor function of the pectoral girdle `muscular sling in trotting dogs. *Journal of Experimental Biology*, 209(11), 2224-2237. doi:10.1242/jeb.02236
- 23) Carrier, D. R., Deban, S. M., & Fischbein, T. (2008). Locomotor function of forelimb protractor and retractor muscles of dogs: Evidence of strut-like behavior at the shoulder. *Journal of Experimental Biology*, 211(1), 150-162. doi:10.1242/jeb.010678
- 24) Lee, D. V. (2011). Effects of grade and mass distribution on the mechanics of trotting in dogs. *Journal of Experimental Biology*, 214(3), 402-411. doi:10.1242/jeb.044487
- 25) Lee, D.V., Bertram, J.E., and Todhunter, R.J. (1999). Acceleration and balance in trotting dogs. *Journal of Experimental Biology*, 202, 3565-3573
- 26) Granatosky, M. C., Fitzsimons, A., Zeininger, A., & Schmitt, D. (2017). Mechanisms for the functional differentiation of the propulsive and braking roles of the forelimbs and hindlimbs during quadrupedal walking in primates and felines. *The Journal of Experimental Biology*, 221(2). doi:10.1242/jeb.162917
- 27) Gray, J. (1944). Studies in the mechanics of the tetrapod skeleton. *Journal of Experimental Biology* 20, 88-116
- 28) Bertram, J. E.(ed.) (2016). *Concepts in locomotion: Levers, struts, pendula and springs*. In *Understanding mammalian locomotion: Concepts and applications* (pp. 79-110). Hoboken, New Jersey: John Wiley & Sons, Inc.
- 29) Haxton, H. A. (1947). Muscles of the pelvic limb. A study of the differences between bipeds and quadrupeds. *The Anatomical Record*, 98(3), 337-346. doi:10.1002/ar.1090980304
- 30) Lee, D. V. (2004). Effects of mass distribution on the mechanics of level trotting in dogs. *Journal of Experimental Biology*, 207(10), 1715-1728. doi:10.1242/jeb.00947

- 31) Deban, S. M., Schilling, N., & Carrier, D. R. (2011). Activity of extrinsic limb muscles in dogs at walk, trot and gallop. *Journal of Experimental Biology*, 215(2), 287-300. doi:10.1242/jeb.063230
- 32) Walter, R. M., & Carrier, D. R. (2011). Effects of fore-aft body mass distribution on acceleration in dogs. *Journal of Experimental Biology*, 214(10), 1763-1772. doi:10.1242/jeb.054791
- 33) Walter, R. M., & Carrier, D. R. (2009). Rapid acceleration in dogs: Ground forces and body posture dynamics. *Journal of Experimental Biology*, 212(12), 1930-1939. doi:10.1242/jeb.023762
- 34) Heglund, N.C. (1981). A simple design for a force-plate to measure ground reaction forces. *Journal of Experimental Biology* 93, 333-338
- 35) Shine, C.L. (2016). *Ursidae locomotion: Right down to the "bear bones"* (Doctoral dissertation). Available from ProQuest Dissertations & Theses Global. (Order No. 10137483)
- 36) Measurements Group, Inc., Technical Staff (1988), *Strain gage based transducers: Their design and construction*. Retrieved from http://amet-me.mnsu.edu/userfilesshared/Equipment_Manuals/TE_110/StrainGageBasedTransVishay.pdf
- 37) Voss, K., Galeandro, L., Wiestner, T., Haessig, M., & Montavon, P. M. (2010). Relationships of Body Weight, Body Size, Subject Velocity, and Vertical Ground Reaction Forces in Trotting Dogs. *Veterinary Surgery*, 39(7), 863–869. doi: 10.1111/j.1532-950x.2010.00729.x
- 38) Taylor, R. J. F. (1957). The work output of sledge dogs. *The Journal of Physiology*, 137(2), 210–217. doi: 10.1113/jphysiol.1957.sp005807
- 39) Almeida, R. A., Vaz, D. C., Urgueira, A. P., & Borges, A. J. (2012). Using ring strain sensors to measure dynamic forces in wind-tunnel testing. *Sensors and Actuators A: Physical*, 185, 44-52. doi:10.1016/j.sna.2012.07.024
- 40) Schilling, N., Fischbein, T., Yang, E. P., & Carrier, D. R. (2009). Function of the extrinsic hindlimb muscles in trotting dogs. *Journal of Experimental Biology*, 212(7), 1036–1052. doi: 10.1242/jeb.020255